

CHAPTER 33

Peripheral Vascular Ultrasound

Ricardo Benenstein, Muhamed Saric

Snapshot

➤ Ultrasound Diagnosis of Carotid Artery Diseases

➤ Ultrasound Diagnosis of Femoral Access Complications

INTRODUCTION

Atherosclerosis is a systemic disease of the medium and large arteries. It affects not only the coronaries—the main focus of cardiologists—but also aorta, carotids, and other major peripheral vessels. It is a dynamic disease that makes prevention and treatment a highly complex process, and it is the leading cause of cardiovascular morbidity and mortality worldwide.

Physicians who fashion themselves as providers of health care to people with cardiac illnesses, frequently encounter patients who may have sought their expertise for treatment of ischemic heart disease but whose lives are also affected by peripheral vascular disease. Thus, there is an increasing trend for these practitioners—who, if board-certified, are deemed experts in “cardiovascular diseases”—to be more involved in the vascular medicine component of their subspecialty. The rapid growth in percutaneous peripheral vascular interventions has contributed to this trend. With the fast pace of noninvasive imaging technology, there has been burgeoning interest among cardiologists, and particularly echocardiographers, in performing vascular ultrasound studies, in an attempt to refine both risk stratification and the need for more aggressive preventive strategies.^{1,2} Furthermore, there is a growing desire among cardiology trainees to acquire more experience in vascular medicine and vascular imaging

modalities. The effort to strengthen the understanding of vascular diseases among cardiologists is reflected in a recent joint statement by the Society for Cardiovascular Angiography and Interventions and the Society of Vascular Medicine: “The essentials of vascular medicine should be taught to all cardiology fellows. Vascular medicine training should be integrated into the fellowship program and include the evaluation and management of vascular diseases, exposure to noninvasive diagnostic modalities, angiography, and peripheral catheter-based interventions.”³

In our experience at the New York University Langone Medical Center’s Noninvasive Cardiology Laboratory, two areas of vascular ultrasound use have fostered particular interest among clinical and interventional cardiologists—the assessment of the extracranial cerebrovascular circulation and the evaluation of complications of femoral access during percutaneous interventions. Both topics will be discussed in detail in this chapter.

ULTRASOUND DIAGNOSIS OF CAROTID ARTERY DISEASES

Introduction

In the United States, stroke ranks as the third leading cause of death, after ischemic heart disease and cancer, and is the

leading cause of permanent disability. Every year, there are >700,000 new stroke cases in the United States, resulting in >150,000 deaths. The economic burden imposed on society, estimated to be more than \$58 billion in direct and indirect costs annually, is enormous.

Carotid artery occlusive disease accounts for 15–20% of the ischemic strokes, of which three quarters involve the anterior carotid circulation and the remaining quarter the posterior vertebrobasilar system. Because most of these cerebrovascular accidents, resulting in significant morbidity and mortality, occur without any warning sign, attention has turned to the detection and management of asymptomatic carotid stenosis, the prevalence of which is on the rise.⁴

The overall prevalence of asymptomatic carotid artery disease (defined as >50% luminal reduction by duplex ultrasound) varies considerably. In the general population, it is between 2% and 8%. But among patients with known coronary artery disease, the prevalence is reported to be 11–26%. It is even higher in patients with recognized peripheral vascular disease.⁵

The risk of stroke is highly dependent on the degree of carotid stenosis and the presence of symptoms. Landmark-randomized multicenter trials have determined that the combination of carotid endarterectomy (CEA) and best medical therapy significantly reduces the risk of stroke in symptomatic patients with $\geq 70\%$ carotid artery stenosis, as well as in asymptomatic patients with $\geq 60\%$ carotid stenosis.^{6–8} At the same time, AbuRahma et al have shown that the heterogeneity of the plaque is more closely related to symptoms than the degree of stenosis, and they have suggested that plaque characteristics be considered when selecting patients for CEA, particularly in asymptomatic carotid disease.⁹

The principal role of carotid duplex ultrasound examination is the detection of stenosis in the internal carotid artery (ICA). But, because of studies demonstrating the prognostic significance of plaque morphology, characterizing plaque by analyzing the gray-scale appearance of the arterial wall, with particular attention to the ultrasonic features of the plaque in the carotid bulb, has important implications. At the same time, the fact that no diagnostic method has been proven to predict which asymptomatic plaques will lead to cardiovascular events makes carotid duplex ultrasound a fertile ground for research in patients with cardiovascular disease.¹⁰

This chapter will emphasize fundamental aspects of the carotid ultrasound examination, including cerebrovascular anatomy and physiology, scanning protocol,

intima-media thickness (IMT) and plaque characterization, criteria for grading stenosis of native arteries, and standards for follow-up evaluation of vessels after endarterectomy and stenting. It should be noted that the accuracy of carotid duplex studies depends on the technical skills of the sonographer, on consistent adherence to the examination protocol, and on the experience of the physician interpreting them.

Cerebrovascular Anatomy

Thorough knowledge of the anatomy of the cervical arteries, including vessel origin and trajectory, branches, and main collateral pathways, is paramount to understanding cerebrovascular hemodynamics, particularly when there is significant stenosis or total occlusion of one the carotid and/or vertebral arteries (VAs). What follows is a basic overview of the cervical arteries and the complex intracranial connections between the anterior and posterior circulations through the Willis circle and main collateral pathways.

Four vessels supply the brain: two internal carotid arteries, which provide circulation to the anterior cerebrum; and two VAs, which provide circulation to the posterior brain. Distally, both circulations join at the base of the brain forming an arterial loop known as the Circle of Willis.

The presence of significant flow abnormalities of the origin of the carotid or subclavian arteries (SAs) will have great impact on the Doppler spectrum and direction of the flow in the cervical arteries. Therefore, knowledge of the anatomy and ultrasound interrogation techniques of the aortic arch vessels is necessary to ensure complete assessment and understanding of the duplex findings.

Aortic Arch

The aortic arch is approximately 4–5 cm long and 2.5–3.0 cm in diameter. Morphologically, the aortic arch is classified as one of three types, based on its relationship to the innominate artery. This assessment, however, is more important to the interventionalist than to the vascular technologist performing ultrasound examination.¹¹

In type I aortic arch, all three great vessels originate in the same horizontal plane as the outer curvature of the aortic arch.

In the type II aortic arch, the innominate artery originates between the horizontal planes of the outer and inner curvatures of the arch.

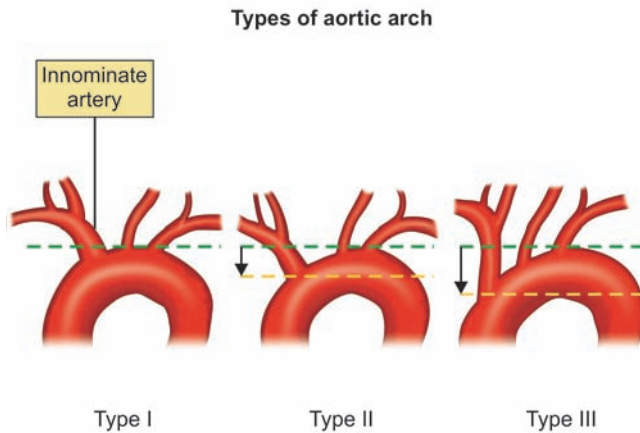


Fig. 33.1: Types of aortic arch. Type I aortic arch—all three great vessels originate in the same horizontal plane as the outer curvature of the aortic arch. Type II aortic arch—the innominate artery originates between the horizontal planes of the outer and inner curvatures of the arch. Type III aortic arch—the innominate artery originates below the horizontal plane of the inner curvature of the arch.

Courtesy: Illustration created by Melissa LoPresti and Robert Spencer, NYU).

In the type III aortic arch, the innominate artery originates below the horizontal plane of the inner curvature of the arch (Fig. 33.1).

The arch gives rise to three great vessels. From right to left, the first branch is the innominate or brachiocephalic artery, which in turn branches into the right SA and the right common carotid artery (CCA). In approximately 70% of the population, the second branch is the left CCA, and the last branch is the left SA (Figs 33.2A to C).

The remaining 30% of the population exhibit any of the several anatomical variations, which may lead to difficulty in the identification of a stenotic vessel.¹²

The most common variant, seen in nearly 15% of the population, is the so-called bovine arch in which the innominate artery and the left CCA share a common origin. Anecdotally, the term bovine arch is a misnomer, as this type of branching is actually exceedingly rare or perhaps nonexistent among cattle (a true bovine aortic arch has no similarity to any of the common human aortic arch variations: the aortic arch branching pattern found in cattle has a single brachiocephalic trunk arising from the aortic arch, which ultimately splits into the bilateral SAs and a bicarotid trunk)¹² (Figs 33.3A and B).

The second most common variant, seen in approximately 10% of the population, involves the left

CCA originating directly from the innominate artery at a distance of 1–2.5 cm from the aortic arch (this variant is similar to the common origin variant, except that the left CCA originates more distally from the innominate artery, rather than as part of a common trunk).¹²

A much less common aortic arch anomaly is a left aortic arch with an aberrant right SA that arises from the arch distally, near the origin of the left SA, and crosses in the posterior mediastinum, usually behind the esophagus, on its way to the right upper extremity (0.5–2.0% of the aortic arch anomalies). When an aneurysmal dilatation of the proximal portion of the aberrant right SA is present, the pouch-like aneurysmal dilatation is called a diverticulum of Kommerell. A similar aneurysm can be seen with an aberrant left SA associated with a right aortic arch.¹³

More rare aortic arch anomalies are beyond the scope of this chapter. The innominate or brachiocephalic artery is the first and largest aortic arch branch. It originates near the midline and travels superiorly and slightly posteriorly toward the right supraclavicular fossa (from where it is best interrogated by Doppler ultrasound). It divides, about 4–5 cm after its origin and just above the right sternoclavicular junction, into the right SA and the right CCA.

The left CCA is the second branch of the aortic arch. It too originates within the thorax immediately after the innominate artery, running anteriorly toward the left side of the neck. Its origin can be evaluated from either the suprasternal notch or the left supraclavicular fossa.

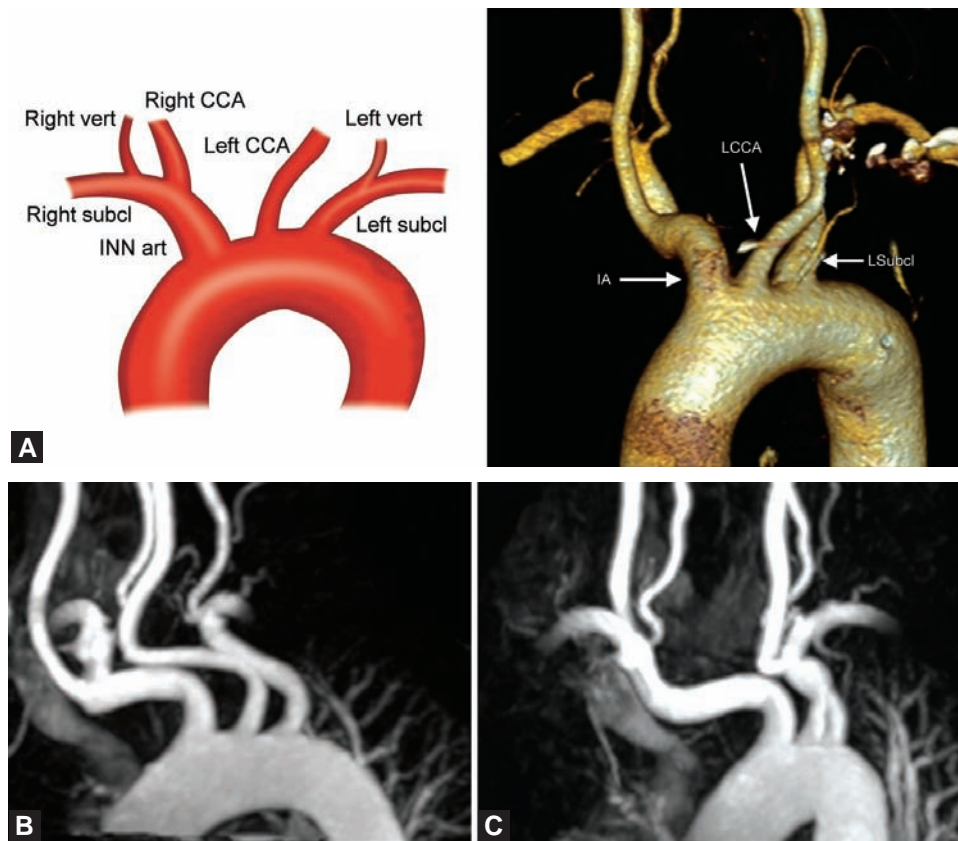
The left SA is the last arch branch; it originates laterally and posteriorly to the left common carotid, and ascends through the thoracic outlet. Its origin is usually interrogated from the left supraclavicular fossa.

Anterior Circulation

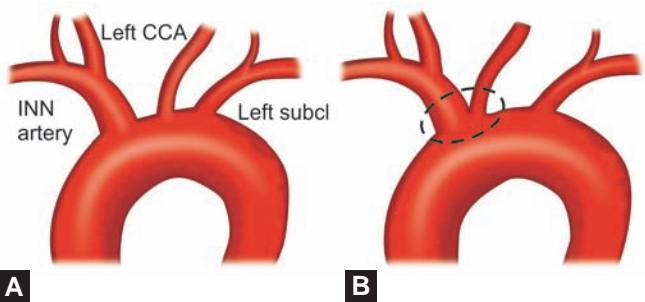
Both CCAs ascend straight through the neck behind the sternocleidomastoid muscles, usually posterior and medial to the internal jugular veins. But their trajectories can become quite tortuous with age and long-standing hypertension.

The CCAs are 6–8 mm in diameter. Generally speaking, they do not give rise to branches proximal to the bifurcation; but it is not uncommon to see the superior or inferior thyroid arteries arise from the CCA near the origin of the external carotid arteries.

The CCA bifurcates into the ICA and the external carotid artery (ECA) at the level of C4 to C5 in approximately 50% of patients. In 10% of patients, this bifurcation is lower in the



Figs 33.2A to C: Branches of the aortic arch. (A) Three-dimensional (3D) volume rendering computed tomography angiography (CTA) demonstrates the normal origin of the great vessels. From right to left: the innominate artery, which in turn branches into the right subclavian and common carotid arteries, the left CCA, and the left subclavian artery. This common variant is present in approximately 70% of the population; (B and C) Magnetic resonance angiography images demonstrate the origin of the great vessels from an anterolateral view (B) and from an anterior view (C). (CCA: Common carotid artery; INN art: Innominate artery; Subcl: Subclavian artery; Vert: Vertebral artery).



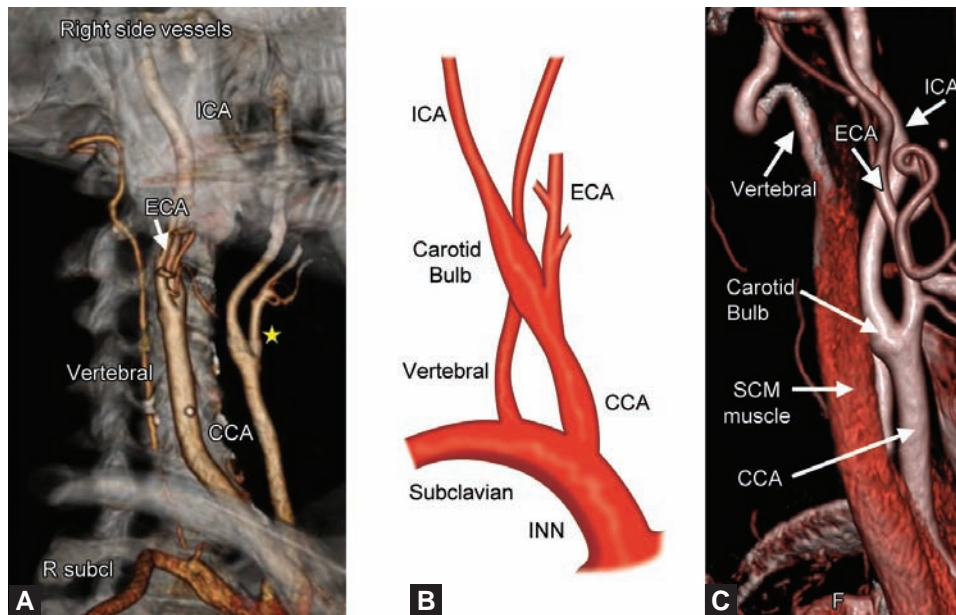
Figs 33.3A and B: “Bovine Arch.” (A) Demonstrates the most common configuration of the aortic arch; (B) The innominate artery and the left common carotid artery share a common origin. This variant is present in 15% of the population and is so-called “Bovine Arch”. This term in fact is a misnomer, as this type of branching is actually extremely rare among cattle.

Courtesy: Illustration created by Melissa LoPresti and Robert Spencer, NYU).

neck (lowest seen at T1–T2), and in about 40% of patients, the bifurcation is higher (highest seen at C1–C2).^{14,15} This variance presents a diagnostic challenge for the vascular technologist performing duplex interrogation of the ICA (Figs 33.4A to C).

The ECA originates at the bifurcation and supplies blood flow to neck, face, scalp, maxilla, and thyroid. It courses superiorly and anteriorly, and gives off a highly variable number of branches before it divides into the maxillary artery and superficial temporal artery. Both terminal vessels are important as collateral pathways, providing known pre-Willisian extracranial–intracranial anastomoses between the ECA and ICA (discussed later in this chapter).

The ICA runs cranially, posterior and lateral to the ECA, and supplies blood to the anterior cerebral hemispheres as well as the ipsilateral eye.



Figs 33.4A to C: Right side vessels. (A) This three-dimensional (3D) volume rendering computed tomography angiography (CTA) demonstrate the relationship of the CCA and the vertebral artery on the right side. The common carotid runs anteriorly behind the sternocleidomastoid muscle, until it bifurcates into the internal and external carotid arteries. The vertebral artery runs posterior and lateral to the common carotid and ascends in the neck within the transverse foramina of the cervical vertebrae C6 to C2. The right subclavian artery originates from the innominate artery bifurcation and runs behind the clavicle bone toward the arm. Indicated with a “star” is the left carotid system. 3D reconstruction courtesy of NYU Langone Medical Center Radiology Lab; (B) Diagram showing the origin and relationship of the anterior and posterior circulations; (C) 3D volume rendering CTA of the CCA and bifurcation. The proximal ICA presents its bulbous, fusiform dilatation known as the “carotid bulb”. (CCA: Common carotid artery; ECA: External carotid artery; ICA: Internal carotid artery; INN: Innominate artery; SCM: Sternocleidomastoid muscle).

Courtesy: Illustration created by Melissa LoPresti and Robert Spencer, NYU).

Typically, the ICA is larger than the external, and its proximal portion has a fusiform dilatation known as the “carotid bulb” because of its particular shape (Figs 33.5A to C).

The carotid bulb begins at the level of the CCA bifurcation and extends 1.5–2 cm into the ICA measuring approximately 7–9 mm in its larger diameter. This structure, known also as the carotid sinus, is heavily innervated, and contains baroreceptors involved in arterial blood flow regulation. In the posterior aspect of the carotid bulb, there is a small cluster of chemoreceptors known as the carotid body, which is responsible for sensing changes in pH, temperature, partial pressure of O_2 , and CO_2 .

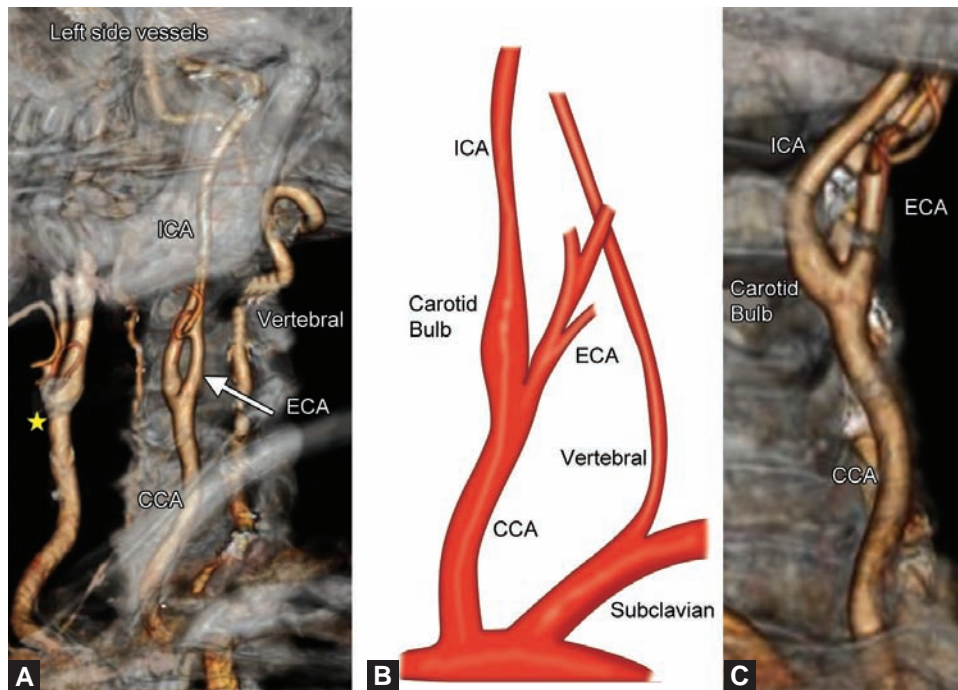
The carotid bulb is the most common site of atheroma formation in the cervical segment of the ICA. The atherosclerotic disease process, as well as revascularization techniques (either surgical or endovascular), may affect the regulatory functions of the carotid bulb.

Distal to the bulb, the ICA is generally straight and measures 4–6 mm in diameter. This vessel turns medially before entering the carotid canal in the petrous bone. The

mid and distal cervical segments of the ICA tend to have only mild curvatures, but it is not uncommon for the ICA to undergo some elongation and to become tortuous with aging or in the presence of hypertension. Three morphological variants may be present:^{15,16}

- Loops are described as “S” or “C” shaped elongations or curved arteries.
- Coils are pronounced, redundant “S” shaped curves (or complete circle of the vessel). Loops and coils are thought to be congenital variations. They are usually bilateral and do not cause symptoms unless exaggerated by aging or aggravated by atherosclerotic disease.
- Kinks are sharp angulations of the artery, usually causing some degree of luminal narrowing, but rarely producing hemodynamically significant stenosis. Aging, atherosclerosis, and hypertension are considered predisposing factors (Figs 33.6 and 33.7 and Movie clip 33.1).

The ICA enters the carotid canal in the temporal bone without giving off any branches in its cervical extracranial



Figs 33.5A to C: Left side vessels. (A) The left common carotid and left subclavian have independent origin in the aortic arch. Three-dimensional (3D) reconstruction courtesy of NYU Langone Medical Center Radiology Lab; (B) Diagram shows the origin and relationship of the anterior and posterior circulations; (C) 3D volume rendering computed tomography angiography (CTA) of the CCA and bifurcation. The carotid bulb is evident in this view. (CCA: Common carotid artery; ECA: External carotid artery; ICA: Internal carotid artery).
Courtesy: Illustration created by Melissa LoPresti and Robert Spencer, NYU).

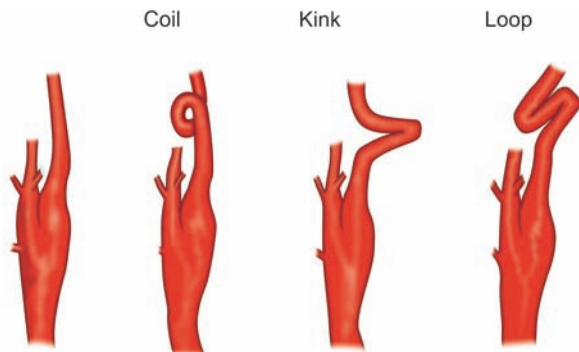


Fig. 33.6: Morphological variants of internal carotid artery (ICA) elongation and tortuosity. Diagram demonstrates the three most common types of curvatures and tortuosity of the ICA.
Courtesy: Illustration created by Melissa LoPresti and Robert Spencer, NYU).

segment. The ophthalmic artery and the posterior communicating artery are the main intracranial branches of the ICA. Both constitute critical collateral pathways in the setting of significant stenosis or total occlusion of the cervical ICA.

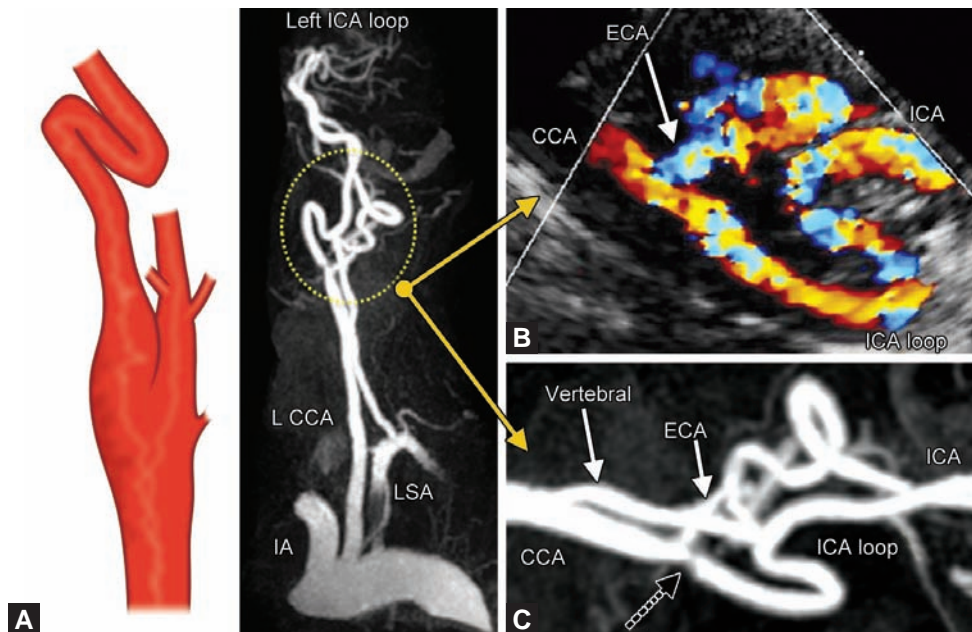
After a short segment known as the supraclinoid ICA, the artery divides into the anterior cerebral artery

and the middle cerebral artery, which are part of the Circle of Willis.

Posterior Circulation

The VAs arise from the posterosuperior aspect of the SAs, and they ascend in the neck within the transverse foramina of the cervical vertebrae C6 to C2—producing a characteristic imaging during color duplex interrogation—before entering the cranium through the foramen magnum. VAs are frequently asymmetric. In 50% of cases the left VA is larger and dominant, in 25% the right VA is larger, and in the remaining 25% they are codominant. In a small fraction of patients, one of the vessels is hypoplastic or even absent.¹⁷

The basilar artery is a short vessel formed by the convergence of the intracranial segments of both VAs, at the base of the medulla oblongata, and which then courses the median groove of the pons. The posterior inferior cerebellar arteries and the anterior inferior cerebellar arteries—branches of the vertebral and basilar arteries, respectively—provide blood flow to the lower medulla, pons, lower cerebellum, and fourth ventricle.



Figs 33.7A to C: Left ICA loop. (A) Magnetic resonance angiography of the left carotid system demonstrate an “S” loop of the mid-distal ICA (within the yellow dotted circle); (B) Color duplex ultrasound image of the mid-distal ICA “S” loop of the left, obtained with a curvilinear C6-2 MHz transducer array. This large footprint transducer provides a large field of view of the neck. Movie clip 33.1 corresponds to this panel; (C) Corresponding computed tomography angiography (CTA) image of the “S” loop in the same orientation as the ultrasound image. The black dotted arrow indicates a moderate stenosis in the carotid bulb. (ECA: External carotid artery; IA: Innominate artery; ICA: Internal carotid artery; LCCA: Left common carotid artery; LSA: Left subclavian artery).

Ultimately, the basilar artery bifurcates into the posterior cerebral arteries, which supply blood to the brain stem, superior cerebellum, and cerebral cortex.

The anterior and posterior circulations are interconnected at the base of the brain via the posterior communicating arteries, each of which connect its ipsilateral ICA with its ipsilateral posterior cerebral artery^{17,18} (Figs 33.8A and B).

Collateral Pathways

With advanced atherosclerosis, the capacity of the cerebral circulation to distribute flow becomes increasingly compromised. However, whether neurological deficits appear depends partly on how well-developed the built-in reserve cerebral collateral circulation is. The ability of the collateral pathways to supply blood depends not only on the age of the patient but also on the speed of the arterial occlusion. This is because atherosclerotic disease may involve collateral pathways in older individuals; or the collateral vessels may not adapt fast enough in the case of sudden occlusions, such as those resulting from embolism.¹⁹

Several routes for collateral circulation have been described:

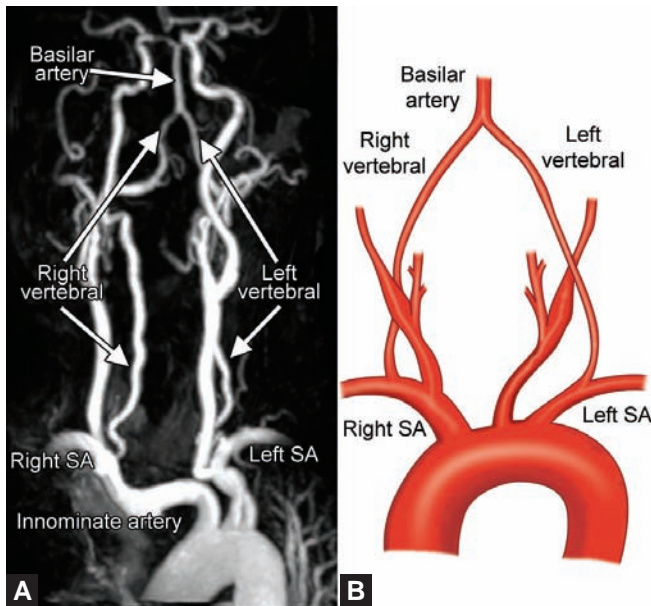
The major intracranial collateral pathway of the brain is the “Circle of Willis.” Thomas Willis (1621–75) is credited with the first description of this structure—a large interarterial connection between the anterior and posterior circulations.

Several possible configurations of the Circle of Willis have been described in the human anatomy, and a complete ring is found in <40% of the patients.

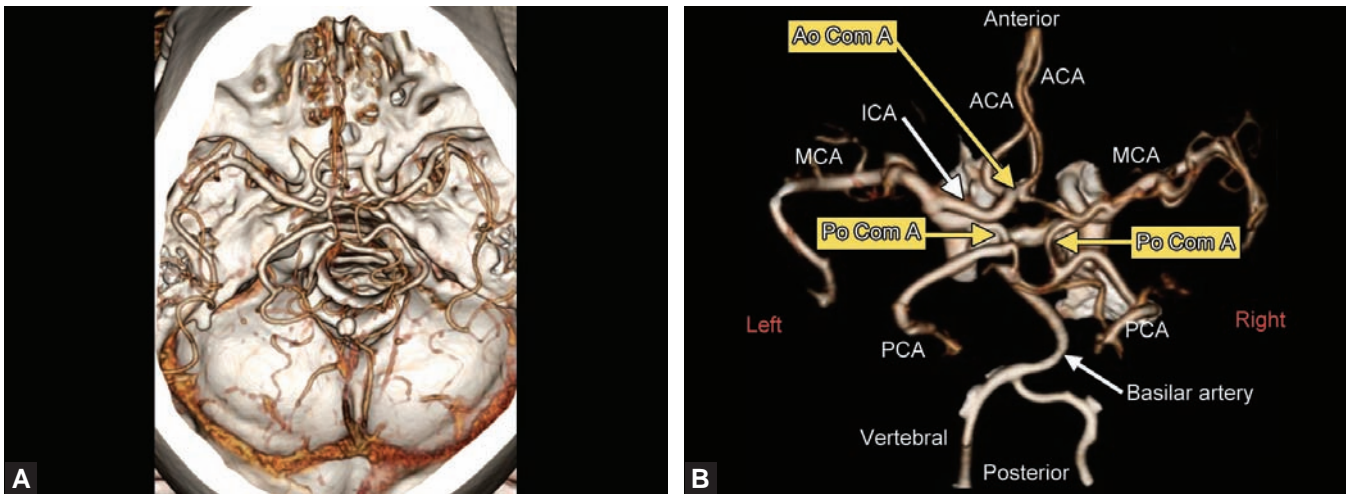
In its most variant form, this arterial ring is created anteriorly by the two ICAs, which give off the anterior cerebral arteries that are then joined by the anterior communicating artery. Both the distal internal carotid arteries are connected to their ipsilateral posterior cerebral artery by the posterior communicating arteries, thus linking the anterior and posterior circulations (Figs 33.9A and B).

There are also important pre-Willisian anastomoses, which play a critical role as collateral pathways in the setting of severe stenosis or occlusion of the ICA:

One of the most important known intracranial-extracranial anastomoses connects the ophthalmic artery (branch of the ICA) to the periorbital branches



Figs 33.8A and B: Posterior circulation. (A) Magnetic resonance angiography of the extracranial and intracranial circulation shows patent vertebral arteries joining together to form the basilar artery; (B) Diagram representing the posterior circulation. *Courtesy:* Illustration created by Melissa LoPresti and Robert Spencer, NYU).



Figs 33.9A and B: Circle of Willis. (A) Three-dimensional computed tomography angiography (3D CTA) reconstruction of the intracranial circulation shows the location of the Circle of Willis at the base of the skull. 3D reconstruction courtesy of NYU Langone Medical Center Radiology Lab. (B) 3D CTA reconstruction with bone suppression demonstrates the configuration of a complete variant of the Circle of Willis. The ICA gives origin to the middle cerebral artery and the anterior cerebral artery in each side. The anterior communicating artery connects both anterior cerebral arteries. The basilar artery divides in the posterior cerebral artery in each side. Two posterior communicating arteries connect the posterior cerebral artery with the ipsilateral ICA, completing in this way the Circle of Willis. 3D reconstruction courtesy of NYU Langone Medical Center Radiology Lab. (Ao Com A: Anterior communicating artery; ACA: Anterior cerebral artery; ICA: Internal carotid artery; MCA: Middle cerebral artery; PCA: Posterior cerebral artery; Po Com A: Posterior communicating artery).

of the superficial temporal artery (branch of the ECA). This anastomosis provides additional blood supply to the ipsilateral distal ICA via reverse flow through the ophthalmic artery.¹⁹

Additional collateral circulation may be found between the occipital branch of the ECA and the atlantic branch of the VA, or cervical branches of the SA and branches of the VA.

In the case of a total occlusion of the innominate artery, the ipsilateral VA can represent a critical collateral pathway to the right common carotid and SAs through retrograde flow in the right VA as it fills from the contralateral vertebral via the basilar artery.²⁰

Technical Aspects of Carotid Studies

An in-depth examination of the extracranial cerebrovascular circulation must include the carotid arteries and the subclavian-vertebral circulation on both sides. The aortic arch and the origin of the great vessels are not ordinarily assessed during a routine exam. However, when Doppler findings suggest significant proximal disease, they ought to be part of the color duplex evaluation and the findings should be reported.

Information about the thickness of the carotid walls, the presence and echographic features of plaques in the carotid bulbs, flow direction, flow velocities in all the interrogated vessels, and assessment of the degree of stenosis by current validated criteria comprise a thorough examination of the cervical arteries, and these should all be reported.

Each laboratory should establish its own scanning protocol to ensure comprehensive examination and accurate reporting, as well as reproducibility among sonographers. The superficial location of the carotid and VAs enables the use of high-frequency linear array transducers (at least 5–7.5 MHz and even higher for analyzing IMT or plaque characterization). Current standard practice includes the use of multifrequency transducers such as a 9–4 or 12–5 MHz probes. State-of-the-art equipment should yield high-resolution B-mode images, color Doppler imaging, and pulsed wave spectral Doppler analysis with angle correction capability.

The study is performed with the patient in the supine position, with his head slightly hyperextended and rotated away from the side being examined to maximize the area of scanning and exposure of the cervical vessels. We recommend the sonographer be seated to the left of the patient, as he does during an echocardiographic examination. The spatial orientation of the monitor should be set to display cranial on the left side and caudal on the right side. Labeling structures is always helpful especially on the transverse views. The sonographer will record static images in B-mode and short video clips (1–3 beats) of color flow mapping and spectral Doppler, illustrating the dynamic changes of the carotid and vertebral flows.

We strongly recommend the use of electrocardiographic recording during the study (as is routine with echocardiographic studies), which facilitates correlation of hemodynamic events with the cardiac cycle [e.g. in patients with an intra-aortic balloon pump (IABP), or in subclavian steal syndrome, etc].

Examples of standardized scanning protocols can be found on the websites of the regulatory commissions for ultrasound studies: the Intersocietal Commission for the Accreditation of Vascular laboratories (ICAVL), the American College of Radiology (ACR), and the American Institute of Ultrasound in Medicine (AIUM).²¹

Scanning Protocol

The following represents the current practice in the Adult Echocardiographic Laboratory at NYU Langone Medical Center. However, laboratories are strongly encouraged to develop their own protocols that best fit their needs and reporting methods (Figs 33.10A to F).

Examination begins with a transverse scan from the base of the neck upward to the lower mandible, with both gray-scale imaging and color flow mapping.

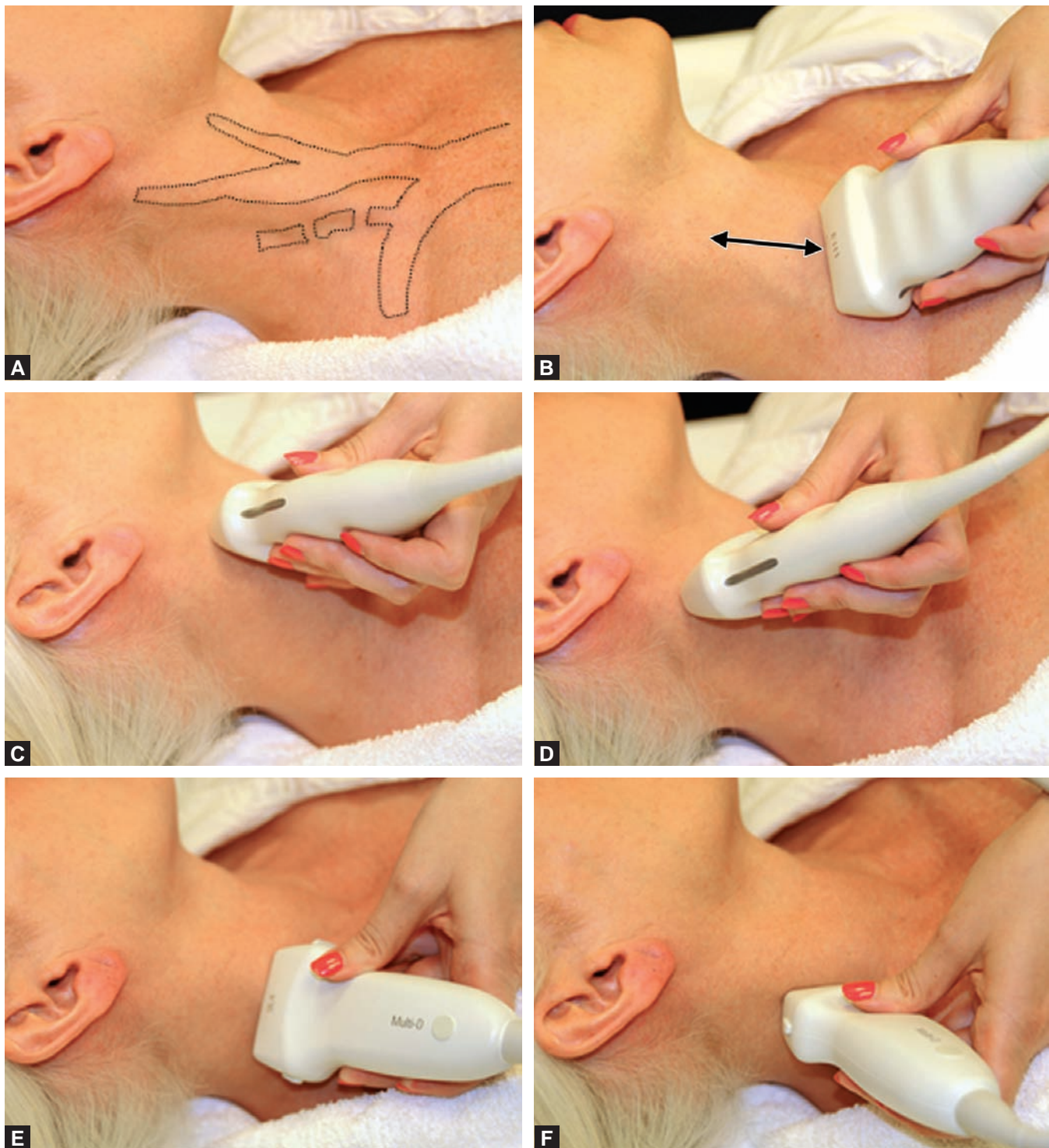
These 6–8 second clips will yield important information regarding the position and patency of the vessels, and the presence or absence of pathology within the carotid arteries (Movie clips 33.2 and 33.3).

The scan is then repeated in the longitudinal view—with both gray-scale imaging and color flow mapping—starting from the very proximal segment of the CCA, moving up to the carotid bifurcation, and then both the internal carotid and external carotid arteries. Particular attention should be paid to the common carotid bifurcation and the carotid bulb, especially if pathology is found at those sites, so that plaque location and extension can be accurately assessed.

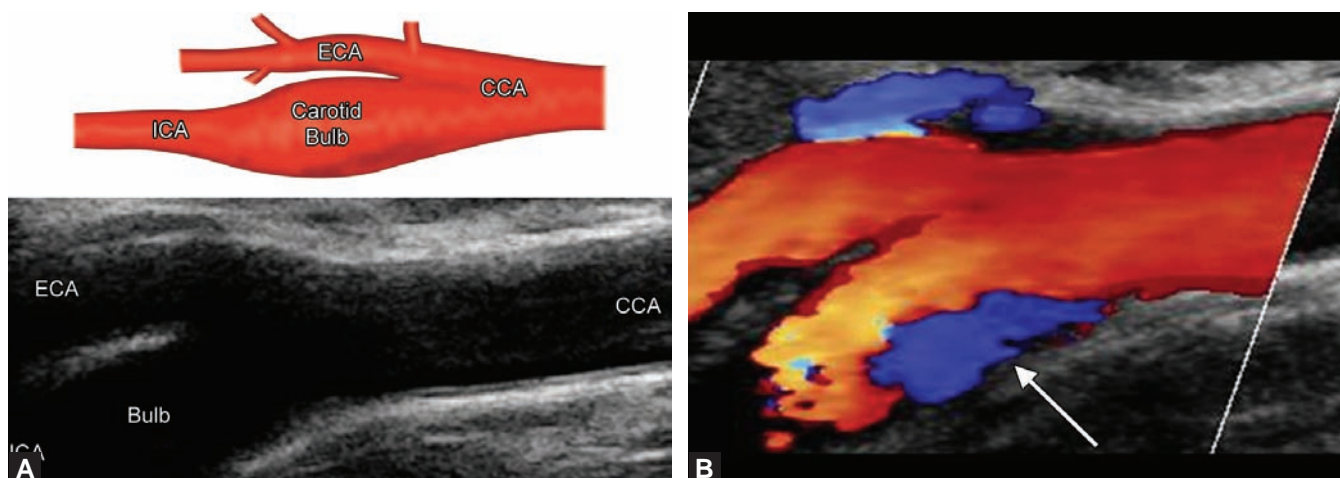
The sonographer will adjust transducer position (anterior, posterolateral, etc.), in order to obtain the most representative views of the cervical arteries. It is important to note that in contrast to echocardiography, there are no specific “standard views” in vascular scanning, so the sonographer’s knowledge of anatomy and pathology, and his technical skills are paramount to ensuring good quality studies and diagnostic results.

The methodology for IMT measurements and plaque characterization will be discussed later in the chapter.

The next step is the pulsed wave Doppler interrogation of each segment and velocity analysis. As with B-mode and color flow assessment, Doppler spectrum analysis should be methodically performed.



Figs 33.10A to F: Duplex scanning protocol. The neck of the patient should be well exposed and the head slightly tilted to the opposite side as shown in (A). Examination begins with a transverse scan from the base of the neck upward to the lower mandible (B), with both gray-scale imaging and color flow mapping as shown in Movie clips 33.2 and 33.3; (C and D) demonstrate the orientation for the longitudinal scan of the common carotid, external carotid, and internal carotid arteries. Note that in the majority of the patients the internal carotid artery courses posterolateral to the external carotid artery (ECA) as shown in (A and D). The transverse scan and the longitudinal scan of the vertebral artery is demonstrated in (E and F), respectively. The vertebral artery travels posterior to the sternocleidomastoid muscle.



Figs 33.11A and B: The carotid artery. A normal carotid artery bifurcation, free of disease, is shown in (A) and (B). The carotid bulb demonstrates flow separation: a high shear stress area with increased velocity indicated by the white dotted line, and a low shear stress area with low velocities and normal physiological turbulence caused by eddy currents (white solid arrow). Movie clips 33.4 and 33.5 correspond to this panel. 🎥

The CCA velocities are assessed in three segments: proximal, mid, and distal, and the velocities are documented. It is known that the peak systolic velocity (PSV) in the proximal CCA may be 10–20% higher than in the more distal segments. We suggest that either all sites be averaged or preferably that the distal CCA velocity be used when calculating the internal carotid artery/common carotid artery (ICA/CCA) ratio for stenosis assessment.

One of the critical issues during vascular scanning is “angle correction.” This methodology is rarely used in echocardiography, but can be an important source of error in vascular investigation if not properly applied. Because the carotid arteries run parallel to the skin, the angle of incidence of the ultrasound beam has to be rectified during Doppler interrogation. (Recall that in the Doppler shift equation the cosine of the angle is integrated in the formula; and ignoring this discrepancy will lead to an underestimation of the flow velocity at this specific point.) A Doppler angle of 60° or less should be applied parallel to the vessel walls if possible, or parallel to the axis of the flow stream if the vessel walls are not well visualized. There is no definitive consensus among experts whether this angle should be routinely modified to compensate for vessel anatomy (e.g. curvature of the distal ICA, loops, kinks, etc.). We recommend maintaining angle correction between 30° and 60° to obtain consistent results in flow velocity measurements. Angles greater than 60° will produce erroneous higher velocities.

The common carotid bifurcation and carotid bulb are the preferred sites for plaque formation, and deserve our best attention during Doppler investigation. The carotid

bulb is a fusiform dilatation of the proximal ICA with a clear zone of flow separation—a high shear stress area with normal to increased velocity situated in the proximity of the flow divider between the ICA and ECA; and a low shear stress area with low velocity and eddy currents situated in the posterior wall of the carotid bulb (Figs 33.11A and B and Movie clips 33.4 and 33.5). Both areas should be sampled with spectral Doppler, and the highest velocity (in the high shear stress area) is used to calculate the ICA/CCA ratio.

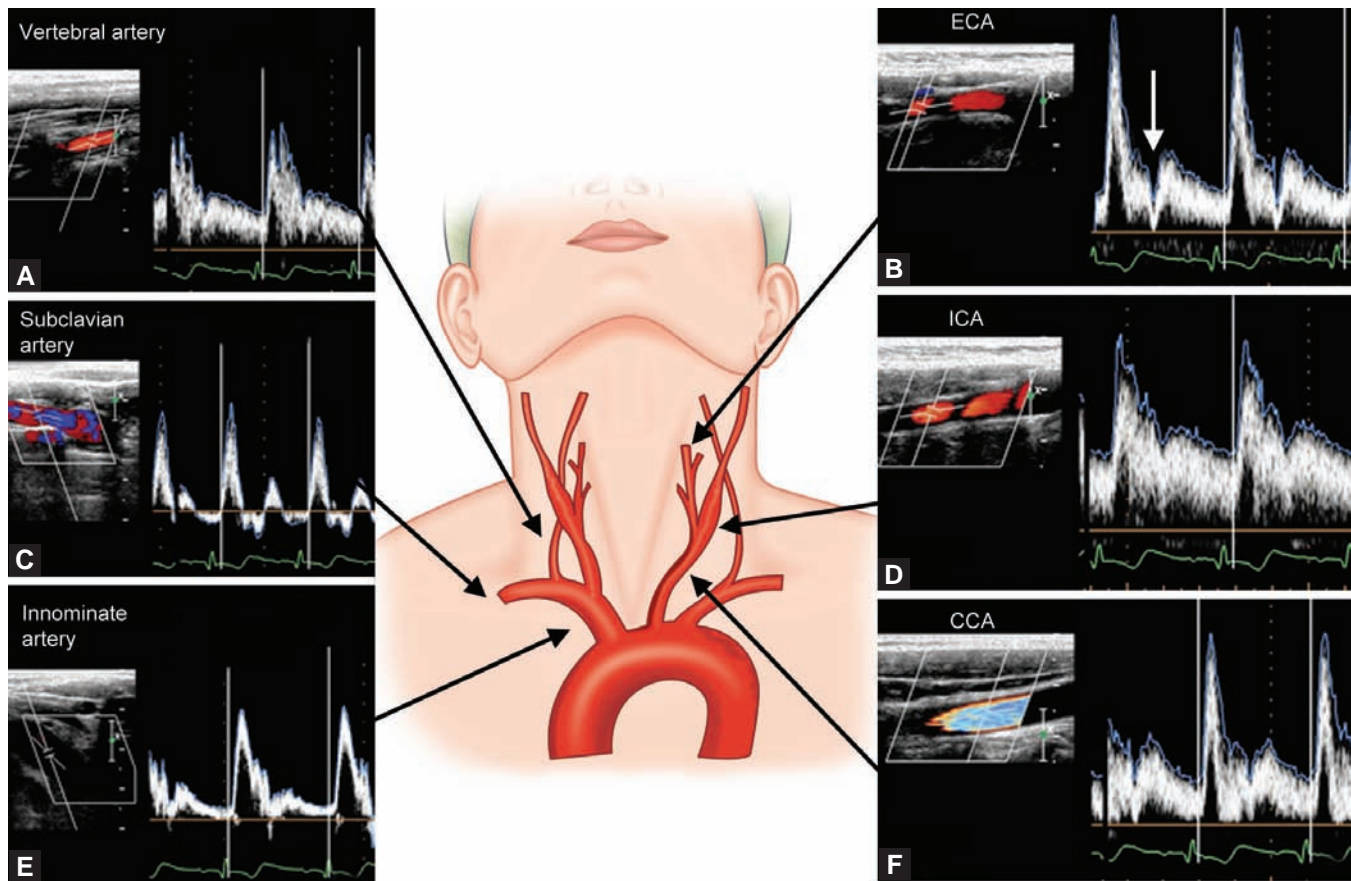
The transducer is then moved cranially, and samples of the proximal, mid, and distal ICA are obtained. The PSV and the end diastolic velocity (EDV) should be recorded and reported, as well as the “dimensionless index” or ICA/CCA ratio.

It is desirable to set the Nyquist limit in the color box between 35 and 45 cm/s to avoid significant aliasing. Color gain will generally be set to approximately 60% and medium-high wall filter to avoid “color bleeding.” These are basic initial parameters that must be tailored to each particular study according to the ultrasound findings.

If focal changes in the hue of the color flow pattern are found (color bruit), this may suggest stenosis that must be evaluated specifically with spectral Doppler.

After thorough examination of the common carotid—internal carotid axis—one or two samples of the ECA should be obtained.

The internal and external carotid arteries are distinguished on the basis of their B-mode appearance (the ICA is larger and includes the fusiform dilated carotid bulb) and their relative position in the neck. The



Figs 33.12A to F: Cervical arteries Doppler spectral waveforms. The ICA and the vertebral artery exhibit a Doppler spectral waveform of low resistance, with significant diastolic flow as shown in (A and D); (B) High resistance spectral waveform of the external carotid artery, characterized by short reversal of flow (white arrow) after a sharp systolic stroke, followed by a lesser degree of forward diastolic flow. The Doppler tracing of CCA reflects the vascular bed of both the internal carotid and the external carotid arteries as shown in Panel F; (C) This is the typical triphasic waveform of the subclavian artery, characteristic of a high-resistance vascular bed (peripheral vessel); (E) The innominate artery Doppler tracing reflects the vascular bed of both the right subclavian artery and the right CCA. (CCA: Common carotid artery; ECA: External carotid artery; ICA: Internal carotid artery).

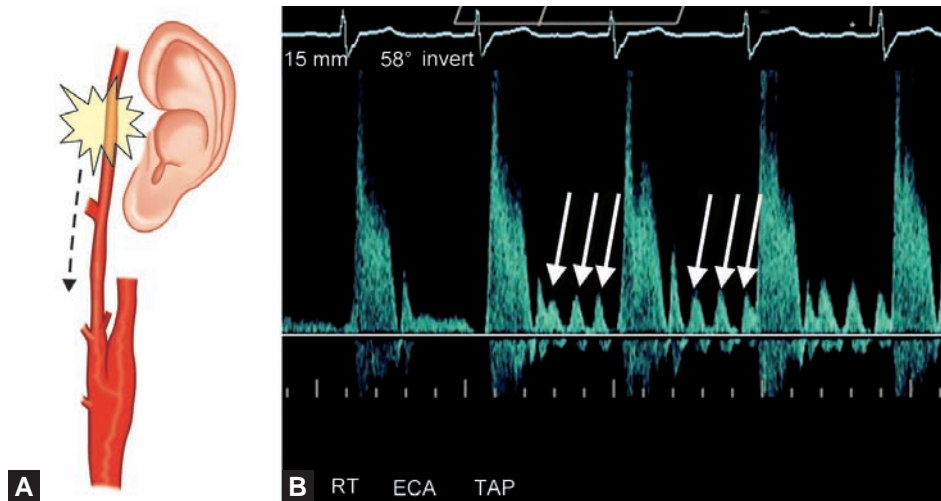
Courtesy: Illustration created by Melissa LoPresti and Robert Spencer, NYU).

ICA courses posterolateral to the ECA in the majority of patients; however, this differentiation is not always easy, especially when there are anatomical variations and when significant pathology is present.

Although they may differ slightly among patients, the spectral waveforms of the common carotid, the internal and external carotid arteries, and the VAs reflect the distal vascular bed supplied by each vessel, and may be used to differentiate the vessels²² (Figs 33.12A to F).

The ICA is larger, travels posteriorly and laterally toward the mastoid process of the temporal bone, and does not give off branches in its cervical portion. The spectral Doppler is of low resistance, exhibiting significant diastolic forward flow.

The ECA is smaller than the ICA, travels anteriorly, and gives off several branches during its passage through the neck. It has a particular spectral Doppler waveform with a short reversal of flow (characteristic of a high resistance distal vascular bed) after a sharp systolic upstroke, followed by a lesser degree of forward diastolic flow. When there is doubt about the identity of the vessels, it is helpful to perform “a temporal tap” maneuver, which consists of a rapid tapping of the preauricular segment of the superficial temporal artery (terminal branch of the ECA), while the ECA is interrogated. This will produce a characteristic fluctuation in the baseline waveform of the artery, confirming its identity. The temporal tap will have little impact in the spectral tracing of the ICA (Figs 33.13A and B).



Figs 33.13A and B: The temporal tap. The temporal tap maneuver helps to identify the external carotid artery. Rapid tapping of the preauricular segment of the superficial temporal artery (A), produces a characteristic fluctuation in the baseline waveform of the external carotid artery indicated by the white arrows in (B).

Courtesy: Illustration created by Melissa LoPresti and Robert Spencer, NYU).

The Doppler tracing of CCA will reflect the vascular bed of both the ICA and ECA, but will more closely resemble the ICA.

As mentioned earlier in this chapter, in about 30 to 40% of patients, the carotid bifurcation is anatomically higher, presenting a challenge for adequately assessing the carotid bulb and distal ICA because of the inability to explore the vessel with a large linear vascular transducer. In this situation, the use of a small footprint transducer (like the sector probe used in transthoracic echocardiography) or a curved array transducer is recommended. Both allow visualization of the artery “hidden” behind the lower mandible. Spectral tracings should be obtained with proper angle correction as described above.

After completing the examination of the anterior circulation, attention should be directed toward the vertebral and SAs.

The VAs travel posterior to the sternocleidomastoid muscles through the foramina of the transverse process of the cervical vertebrae. This produces a typical image of the VAs in the longitudinal plane, characterized by the color flow of the vessel interrupted by the shadow of the bone. The typical Doppler tracing resembles that of the ICA as reflects its downstream to a low resistance vascular bed. One or two Doppler samples of the artery should be recorded. Following the VA inferiorly, it may be possible to find its ostium on a transverse view of the SA.

A transverse scan showing both the common carotid and VAs will yield information regarding directionality of the VA. In the case of the subclavian steal syndrome,

the vertebral will exhibit color flow in opposite direction in systole because of reversal of flow. In the absence of pathology, the common carotid and the vertebral will exhibit the same flow direction in systole and diastole.

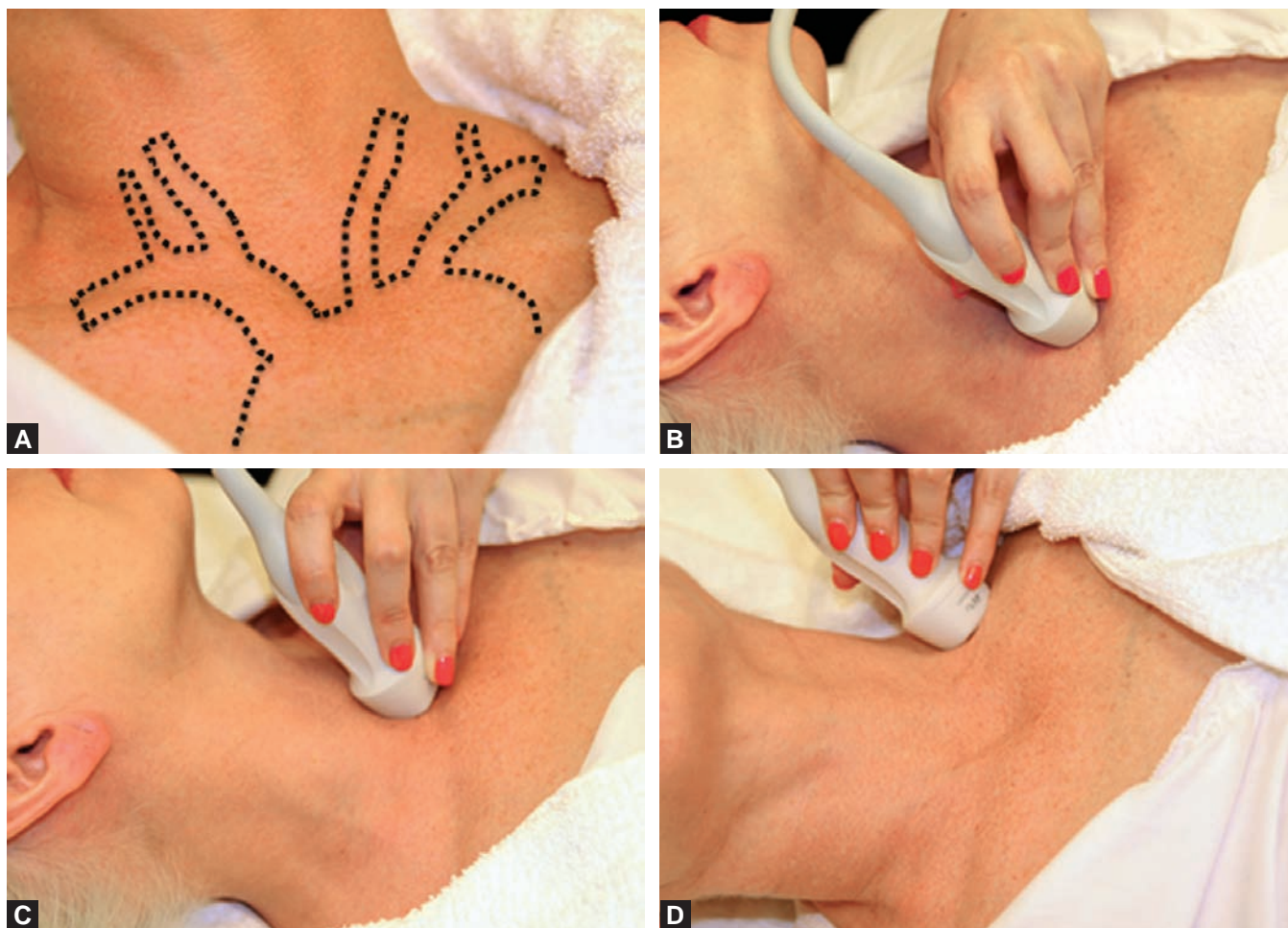
The proximal SA can be interrogated above the clavicle and the distal vessel below the clavicle. The typical Doppler tracing is a triphasic waveform characteristic of a peripheral high-resistance vascular bed.

Any flow disturbance indicative of significant proximal disease (e.g. “parvus and tardus” tracings in the right common carotid and right SAs; reversal of flow in the left VA with “parvus and tardus” waveform in the left SA) should warrant investigation of the aortic arch and the origin of the great vessels. This can be accomplished using a regular transthoracic sector probe to image the aortic arch as is done during a routine cardiac exam.

The innominate artery and its bifurcation are best approached from the right supraclavicular space, directing the transducer downward with a slight anterior tilt.

The left CCA is best visualized from the suprasternal notch, and the origin of the left SA is best visualized either from the suprasternal notch or from the left supraclavicular space. Due to substantial anatomical variations, sonographic access to each vessel will vary from patient to patient (Figs 33.14A to D).

One must again stress the importance of wall thickness measurements and assessment of plaque in the carotid bulb, even in absence of significant hemodynamic compromise. The presence of carotid plaque in the bulb, its size, area, and



Figs 33.14A to D: Aortic arch scanning protocol; (B) The innominate artery and its bifurcation are best approached from the right supraclavicular space, directing the transducer downward with a slight anterior tilt; (C) The left common carotid artery is best visualized from the suprasternal notch or from the left supraclavicular space; (D) The left subclavian artery is best interrogated from the left supraclavicular space. Access to the great vessels may vary significantly from patient to patient due to substantial anatomical variations.

echogenicity have been shown to have strong predictive value for cardiovascular events even in the absence of increased IMT or other conventional risk factors. In this regard, quality data will help to guide medical therapy in those patients.

Intima-Media Thickness and Assessment of Carotid Plaque: Are We There Yet?

Early detection of atherosclerosis and prevention of its progression has become an important goal in medicine. Thus, imaging test capable of quantifying atherosclerotic burden and that could be incorporated into existing risk stratification models might be very useful.

Since the 1980s, there have been wealth of data correlating carotid intima-media thickness (CIMT) with coronary atherosclerosis. However, whether CIMT can

be regarded as a validated marker for cardiovascular risk remains a topic of debate.

CIMT is defined as the “double-line pattern visualized by echotomography on both walls of the CCAs in a longitudinal image. It is formed by two parallel lines, which consist of the leading edges of two anatomical boundaries: the lumen-intima and media-adventitia interfaces.”²³

CIMT has been identified as a sensitive, reproducible imaging technique for detecting atherosclerosis and monitoring its progression and regression.

CIMT measurements and detection of carotid plaque have proven most useful for refining cardiovascular risk assessment in patients with intermediate Framingham risk scores (FRS 6–20%) but without known coronary, cerebrovascular, or peripheral atherosclerotic disease, diabetes, or abdominal aorta aneurysm.²⁴

Other patients who may benefit from CIMT evaluation are those with:

- family history of premature CVD in a first-degree relative;
- individuals with severe abnormalities (e.g. genetic dyslipidemia), who otherwise would not be candidates for pharmacotherapy; or
- women younger than 60 years of age with at least two CVD risk factors.

Imaging should not be performed in patients with established atherosclerotic cardiovascular disease or in whom the results would not be expected to alter therapy.²⁴

It is recommended that CIMT be performed using a high-frequency linear array transducer operating at a fundamental frequency of at least 7 MHz (preferentially 9 MHz and above); this provides an axial resolution that will be smaller than the predicted IMT for the patient, enabling the two echo interfaces to be clearly identified.

Measurements should be made from high resolution gray-scale images along a segment of the distal 1 to 2 cm of the CCA that is at least 10 mm in length—ensuing maximum reproducibility.^{2,24}

Studies have shown that the “far wall” IMT measurements closely represent its true biological thickness; and that of other portions of the CCA, the “near wall” IMT measurements, may be misleading for two reasons: they tend to overestimate the true value of that segment, and the segment itself is less representative of the entire CCA.^{25,26}

Additional measurements may be obtained from the posterior wall of the carotid bulb, and proximal ICA, especially in the absence of plaque. If plaque is present, a detailed description of location, size, echogenicity, and texture is warranted.

Most current state-of-the-art ultrasound systems are equipped with semiautomatic edge-detection software that, when used on high-quality images, tends to improve accuracy and reproducibility, and shorten reading time (Figs 33.15A to C).

Reporting should include the maximum CIMT and calculated mean CIMT for each side, as well as the averages of each value for each side.

CIMT values must be interpreted within the context of patient’s demographic characteristics—age, sex, and race/ethnicity. The results will be communicated by describing ranges of percentiles. This avoids the appearance of greater precision than is achievable when mapping CIMT values to a reference population.

- CIMT values exceeding the 75th percentile are considered to have increased CVD risk.
- Patients whose CIMTs fall within the 25th to 75th percentile are considered to have average CVD risk.
- Those whose CIMTs are lower than the 25th percentile are assumed to have lower CVD risk, but whether this justifies less aggressive preventive therapy is still moot.

Data on changes in IMT over time are scarce, so serial studies to assess progression or regression are currently not recommended.

CCA IMT values and percentiles from large North American and European cohort studies for identifying subclinical vascular disease and evaluating cardiovascular disease risk can be found in the consensus statement from the American Society of Echocardiography.²⁴

Because of the association of increased carotid CIMT with traditional risk factors—such as hypertension, hyperlipidemia, diabetes, and tobacco use—arteriosclerosis is assumed to be its underlying cause.

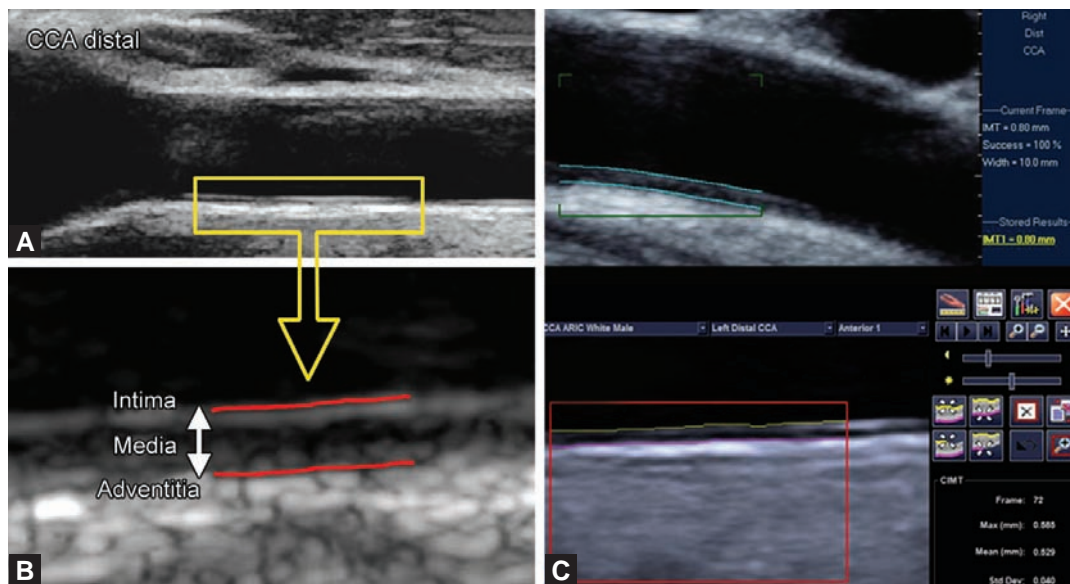
Carotid plaque formation occurs most commonly in atherosclerosis-prone areas of disturbed flow. This manifestation of the atherosclerotic process is typically seen in the posterior wall of the carotid bulb, for example, a site of “low wall shear stress.”²⁶

Large prospective studies and meta-analyses have identified increased CIMT as having prognostic value for cardiovascular events.^{27–31} Others, however, have found that CIMT alone has a weak predictive role.^{32,33}

Thus, cardiovascular risk stratification employing IMT should be comprehensive and include evaluation of multiple carotid segments, as well as the presence and features of plaque.^{26,34}

Several large randomized trials including North American Symptomatic Carotid Endarterectomy Trial (NASCET) and European Carotid Surgery Trial (ECST),^{6,7} have established the criteria for intervention in symptomatic carotid artery stenosis. But management of asymptomatic carotid artery disease remains controversial, as, for example, in Asymptomatic Carotid Atherosclerosis Study (ACAS), which suggested that at least 20 asymptomatic patients had to be treated for 5 years to prevent a single stroke.⁸ It is certainly clear that stenosis alone does not predict which asymptomatic plaque will lead to cardiovascular events.³⁵ Plaque morphology has, therefore, emerged as an additional factor in assessing risk for cardiovascular events.

According to the Mannheim consensus (2004–2006): Plaque is a “focal structure encroaching into the arterial lumen of at least 0.5 mm or 50% of the surrounding IMT



Figs 33.15A to C: Intima-media thickness. (A) A high-resolution gray-scale image of the far wall of distal CCA is obtained and magnified; (B) The magnified image shows the intima-media thickness (IMT) of the far wall of the CCA. A thin layer in the immediate tissue–lumen interface identifies the intima. The media follows as a thicker and hypoechoic layer between the intima and the adventitia. A bright, thick layer separating the vessel wall from the surrounding tissue represents the adventitia; (C) Two samples of semiautomatic edge-detection software from different vendors. (CCA: common carotid artery).

value, or demonstrates a thickness > 1.5 mm as measured from the media–adventitia interface to the intima–lumen interface.”²³

Plaques should be evaluated with high-resolution gray-scale images without color flow mapping. Both longitudinal and transverse views are required to completely assess a plaque’s size and extension.

It is important to determine the location, size and extent of the plaque, as well as its thickness, echogenicity, and texture. The degree of luminal narrowing produced by a plaque’s encroachment should also be assessed.³⁶

Plaques may progress from small intraluminal protrusions lacking any significant hemodynamic effects to high degree stenosis or total occlusion of the vessel.

Larger carotid plaque size is associated with a higher risk of stroke and major adverse cardiovascular events. In a 5-year prospective study of 1,600 patients, Spence et al found an adjusted relative risk of 2.9 for a combined stroke and acute coronary event end point in patients with large carotid plaque area.³⁷

Based on ultrasonographic and histological correlations, plaques that are classified as echogenic have increased calcified and fibrous tissue; and those that are echolucent have higher lipid content, increased macrophage density, and a thin fibrous cap.

Studies have shown that the presence of echolucent (hypoechoic) plaques is highly predictive of stroke and cardiovascular events.^{37–39} In fact, the more echolucent a plaque appears on ultrasound, the more likely the patient will sustain a TIA or stroke in the future.

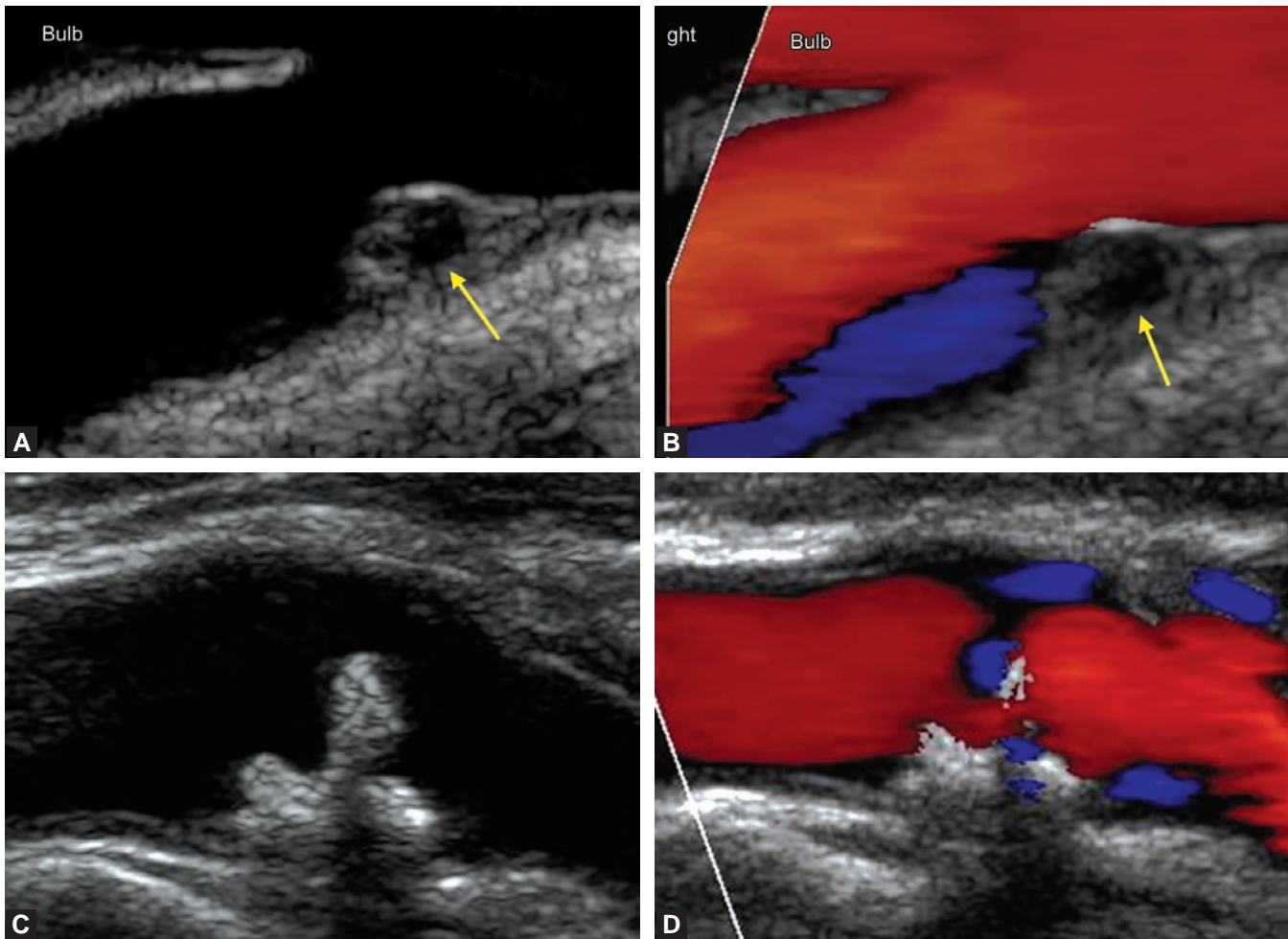
Surface irregularities and intraplaque hemorrhage are characteristics of complicated plaques. While intraplaque hemorrhage is a marker of plaque inflammation and instability, its role as an independent predictor of future ischemic events is not well established³⁵ (Figs 33.16A to D and Movie clips 33.6 and 33.7).

Calcification is very common in carotid plaques. Calcification provides the plaque with structural stability, making it less likely to rupture, and cause symptoms than a noncalcified plaque would be.⁴⁰

Gray-scale images do not reliably identify plaque ulceration. But focal depression associated with irregularities in the plaque’s surface may suggest the presence of an ulcerated plaque, and color Doppler may help to demonstrate the ulceration (Figs 33.17A to F).

The ultrasonic plaque classification used most frequently today is based on the Gray-Weale criteria. Modified by Geroulakos in 1993, is known as the “Geroulakos classification”.⁴¹

Type 1: Uniformly echolucent plaque, with or without a visible thin fibrous cap.



Figs 33.16A to D: Intraplaque hemorrhage and protruding plaque. (A and B) Duplex ultrasound shows a small, nonobstructing echolucent plaque in the carotid bulb, with an anechoic area within (yellow arrow), very suggestive of intraplaque hemorrhage. There is no hemodynamic disturbance of the blood flow as demonstrated by the absence of color flow acceleration and the presence of normal physiological turbulence. Movie clip 33.6 corresponds to this panel; (C and D) Duplex ultrasound shows a heterogeneous, irregular protruding plaque in the carotid bulb in a patient admitted for recurrent transient ischemic attacks. Note in Movie clip 33.7 the mobile component of this plaque. 🎥

Type 2: Predominantly echolucent plaque, < 50% of which contains echogenic areas.

Type 3: Predominantly echogenic plaque, < 50% of which contains echolucent areas.

Type 4: Uniformly echogenic plaque.

Type 5: Unclassified plaque in which heavy calcification and acoustic shadows precludes adequate visualization (Figs 33.18A to F).

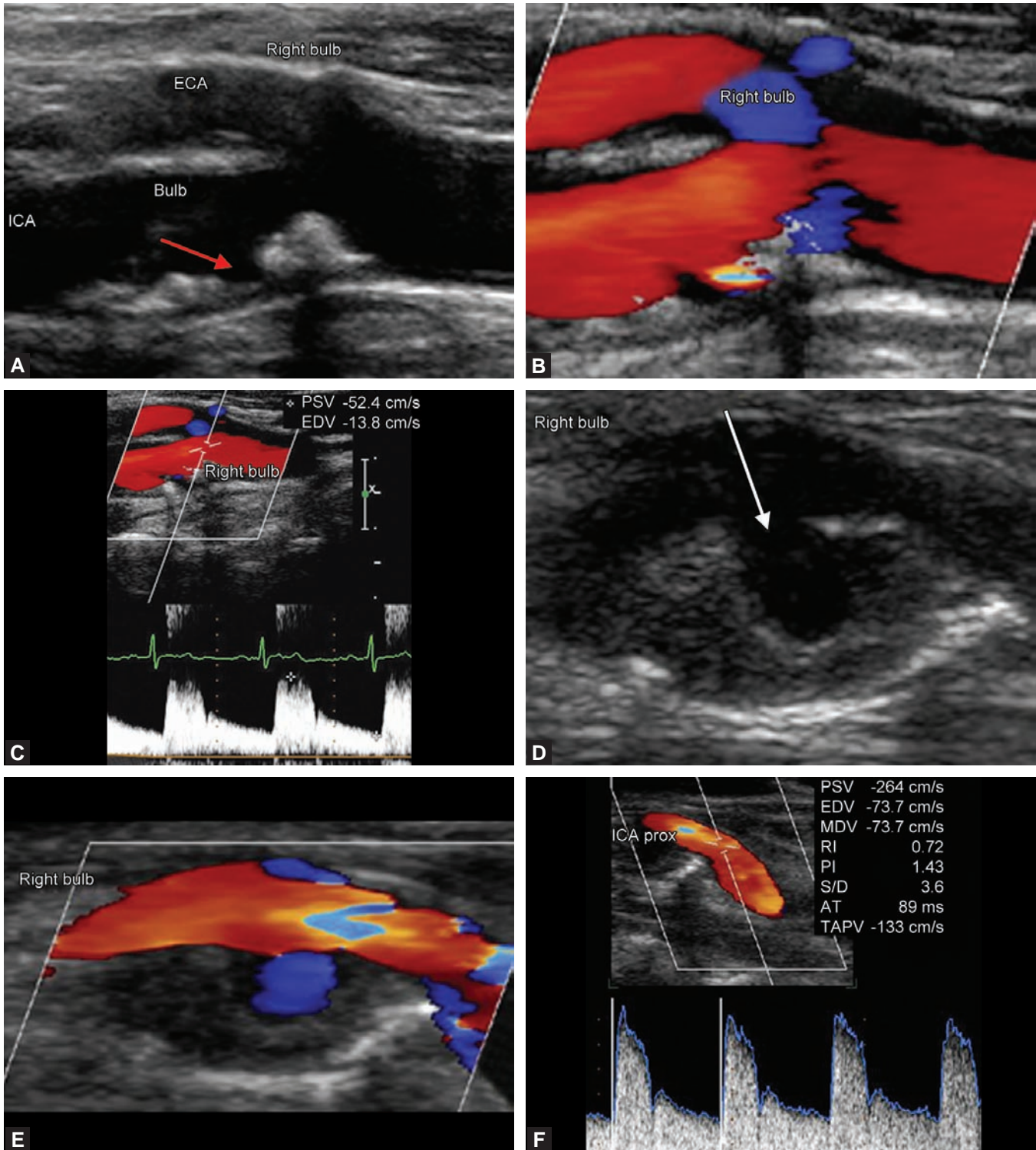
Ultrasound examination and plaque characterization are highly subjective. The use of disparate gain, filter, and compression settings by different operators may result in poor reproducibility. B-mode image normalization by computer-assisted measurements of plaque echodensity has helped to overcome this problem.

For the most part, this innovation remains a research tool used in the identification of vulnerable plaques and in large studies of carotid stenting. But the software is expected to become commercially available for duplex scanners in the near future.

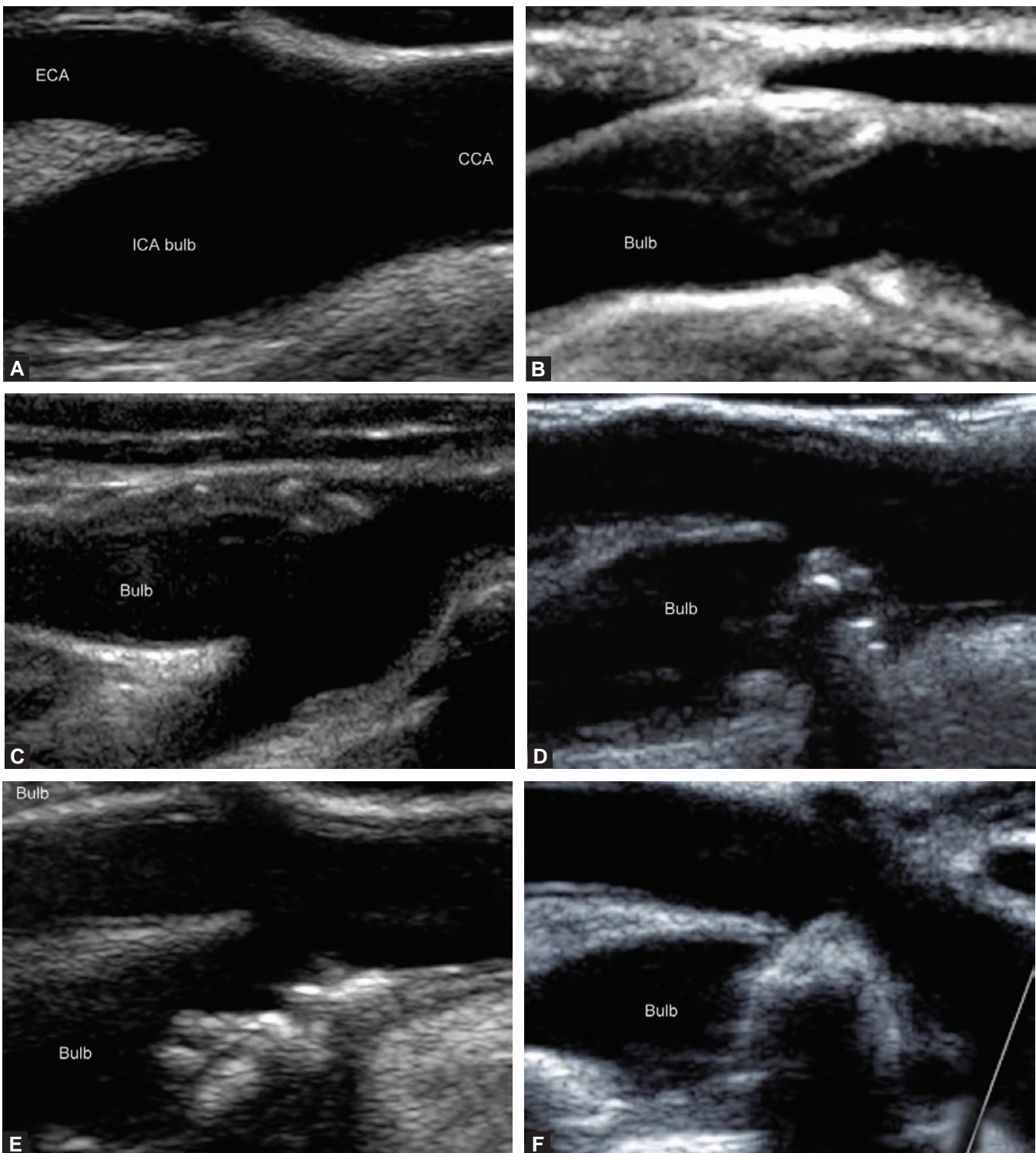
Grading Carotid Stenosis: How much is Severe?

Internal Carotid Artery Stenosis

The criteria for defining a hemodynamically significant ICA stenosis by duplex ultrasound have been debated for decades. Digital angiography is still considered the



Figs 33.17A to F: Ulcerated plaque. (A and B) The gray-scale and color flow images demonstrate a heterogeneous plaque in the posterior wall of the carotid bulb with a focal depression suggestive of ulceration (short red arrow). The color flow imaging helps to demonstrate the ulceration. The Doppler interrogation in (C) demonstrates normal velocities. There is no hemodynamically significant stenosis associated with this plaque; (D) The gray-scale and color flow images show a large, predominantly echolucent plaque in the posterior wall of the carotid bulb, with a deep depression and interruption of the fibrous cap (white long arrow). The color flow fills the cavity in (E), and shows evidence of flow disturbance characterized by a flow convergence (“pisa” flow) in the distal segment of the bulb; (F) demonstrates significant increase in systolic and diastolic velocities, consistent with moderate degree of stenosis.



Figs 33.18A to F: The Geroulakos classification. (A) Normal carotid bifurcation and carotid bulb free of disease; (B) Type 1: Uniformly echolucent plaque, with or without visible thin fibrous cap. (C) Type 2: Predominantly echolucent plaque, <50% of which contains echogenic areas; (D) Type 3: Predominantly echogenic plaque, <50% of which contains echolucent areas; (E) Type 4: Uniformly echogenic plaque; (F) Type 5: Unclassified plaque in which heavy calcification and acoustic shadows precludes adequate visualization.

gold standard for severity assessment, and cardiovascular laboratories must correlate and validate their own criteria against angiograms. However, because routine angiograms to corroborate noninvasive findings are not presently the norm, and the use of computed tomography angiography (CTA) and magnetic resonance angiography for validation is not yet recognized, establishing and validating intrainstitutional duplex criteria may be challenging.⁴²

Several sets of criteria have been published in the last two decades, and clinicians have relied on dissimilar institutional experience for interpreting their own carotid duplex studies. The fact that two distinct angiographic grading systems were used in landmark-randomized trials^{6-8,43} has contributed to the confusion regarding the criteria for assessing ICA stenosis.

One technique—the distal degree of stenosis, also known as the North American or “N” method—defines the residual lumen as a percentage of the normal distal ICA. This method dates back to 1970 when it was believed that hemispheric symptoms were related to flow-limiting lesions. It was used in the NASCET,⁶ and in the ACAS.⁸

The other technique—the local degree of stenosis, also known as the European or “E” method—expresses the residual lumen as a percentage of the original diameter of the carotid bulb. This method was used in the ECST⁷ and by the University of Washington vascular team to develop one of the first duplex velocity criteria for grading internal carotid stenosis.⁴⁴

The shortcoming of the “N” method is that it underestimates plaque size. A diameter reduction of about 40% by a plaque that uniformly affects the wall of the carotid bulb will yield a residual diameter equal to that of the unaffected distal ICA.

In contrast, the “E” approach, which may provide an accurate estimate of plaque size, may not adequately define the location of the plaque because the boundaries of the bulb are not well visualized on angiography. While the University of Washington team used the presence of microcalcifications in unsubtracted angiography films to delineate the carotid bulb, there was great deal of interobserver variability.⁴³

The carotid bulb comprises a normal, but highly variable region of dilatation. Because of its larger diameter, a “stenosis” classified as mild to moderate using the local grading or European method may not be graded as a stenosis at all using the distal quantification or North American method. This disparity using the “N” and the “E” methods is shown in Figures 33.19A to C.⁴³

The figure shows, for example, that a lesion producing a stenosis of 55% by the local grading or European “E” method corresponds to one producing a 0% stenosis by the distal quantification or North American “N” method. This discrepancy between the two methods does little to facilitate the interpretation of carotid duplex findings in relation to the major CEA trials. (The initial duplex velocity criteria developed by Strandness at the University of Washington relied the local degree of stenosis or “E” method. Zweibel later modified the velocity criteria to correspond to the degree of stenosis defined by the “N” or distal stenosis method).^{44,45}

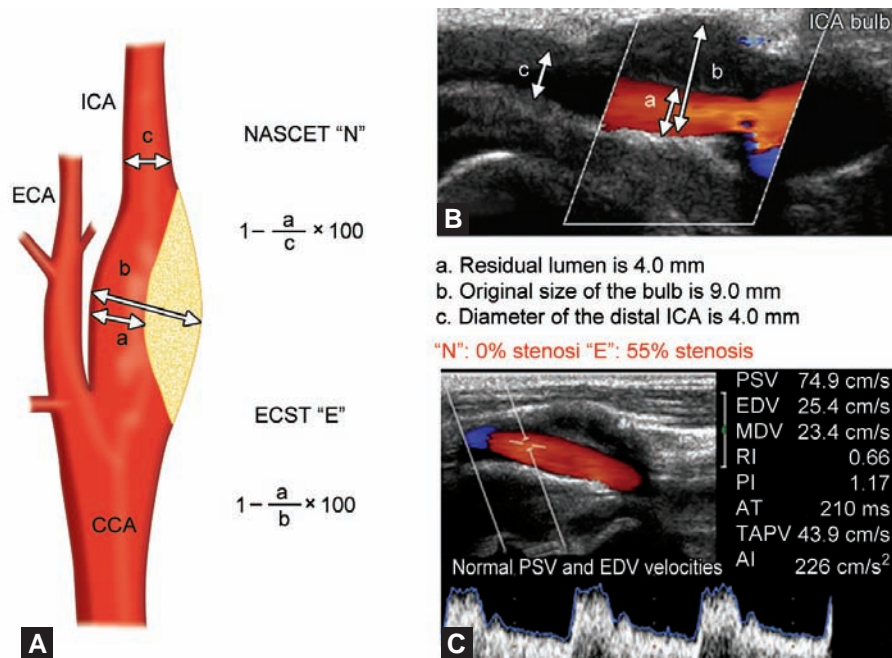
Furthermore, these criteria neglect the fact that the hemodynamic disturbances of a non-flow-limiting lesion are less clinically relevant than the risk of embolism, which is better correlated with the increased thickness, echogenicity, and eccentricity of the plaque.

Therefore, the role of modern carotid duplex ultrasound is not limited to the velocity analysis that has been used to identify which patients will benefit from revascularization therapies. The technique allows us not only to assess the degree of luminal narrowing, but also to evaluate other aspects of carotid disease that are associated with increased risk of stroke and cardiovascular events, such as increased IMT and plaque characterization. This topic will be discussed in more detail later in this chapter.

The advent of accreditation of noninvasive vascular laboratories increased the need for standardization of the criteria to grade the severity of carotid stenosis. In 2002, by initiative of the Society of Radiologists in Ultrasound, a panel of experts met in San Francisco, California to arrive a consensus regarding the diagnosis of carotid artery stenosis by duplex ultrasound. These new criteria were included in the 2006 Guidelines for Noninvasive Vascular Laboratory Testing by the American Society of Echocardiography.^{1,46}

The new consensus criteria use the diameter of the distal unaffected ICA (the “N” method) to assess the degree of carotid stenosis.

The PSV at the site of a significant stenosis depends not only on the pressure gradient across the stenosis, but also on the status of the contralateral carotid artery system, the completeness of the Circle of Willis, and the development of the intracranial-extracranial collateral circulation. It is therefore obvious that for a given degree of angiographic stenosis there will be some discordance with Doppler velocity measurements. To improve the correlation, the classification of stenosis based on duplex velocities was redesigned to create categories (e.g. <50%;



Figs 33.19A to C: Grading ICA stenosis. (A) Shows the difference between the North American or "N" and the European or "E" methods. In the NASCET study, the degree of stenosis (a) is calculated as a percentage of the normal distal ICA (c). In the ECST study, the degree of stenosis (a) is expressed as a percentage of the original diameter of the carotid bulb (b); (B) In this example of a large plaque occupying the carotid bulb, using the "N" method and the "E" method, there is 0 and 55% degree of stenosis (hence the confusion of the readers!). In this particular case, the original size of the bulb (b) appears slightly larger than usual, which makes the difference between methods even more notable; (C) The spectral velocity analysis shows that despite the large occupying plaque in the carotid bulb, there is no hemodynamically significant flow disturbance evident by systolic and diastolic velocities within normal limits. (ICA: Internal carotid artery).

50–69%, >70% stenosis). This, nevertheless, left a great deal of heterogeneity in the moderate range (50–69%).⁴⁷

For physicians accustomed to reading echocardiograms, the assessment of ICA stenosis is similar to the assessment of hemodynamic parameters in patients with aortic valve stenosis.

The main parameters are: tissue characterization (plaque classification); the peak velocity proximal to the stenosis (CCA); the peak velocity at the level of minimum diameter (ICA stenosis); the "dimensionless index" or internal carotid to common carotid peak velocity ratio; and in vascular ultrasound, the EDV at the level of the stenosis.

A complete carotid duplex examination, therefore, should include recording and reporting of the following:

1. IMT measured in the far wall of the distal CCA on both sides
2. If plaque is present, the carotid bulb, images sufficient to describe its localization, extent, thickness, texture, and echogenicity. Images should be obtained in sagittal and transverse scans in gray scale and with color flow Doppler.
3. Spectral Doppler analysis of the vessels in both sides, including peak systolic and end diastolic velocities of

the proximal, mid, and distal CCA; the ICA at the level of the bulb, proximal, mid, and distal segments; the ECA; and the subclavian and VAs.

4. The ICA to CCA peak systolic ratio (the "dimensionless index" of the carotid artery).
5. Flow direction of the VAs (antegrade or retrograde).
6. Doppler interrogation of the great vessels of the aortic arch is not routinely done, unless the hemodynamic findings on the cervical arteries warrant further investigation (e.g. reversal of flow in one of the VAs due to subclavian steal syndrome).

Grading Internal Carotid Artery Stenosis by the Consensus Panel of the Society of Radiologists in Ultrasound⁴⁶ (Table 33.1).

The ICA is considered normal when ICA PSV is < 125 cm/s and no plaque or intimal thickening in the carotid bulb is visible in the two-dimensional (2D) gray-scale images. Additional criteria include ICA/CCA PSV ratio < 2.0 and ICA EDV < 40 cm/s.

Table 33.1: Diagnostic Criteria by the Society of Radiologists in Ultrasound Consensus Panel

	ICA PSV cm/s	Plaque/Diameter	ICA/CCA PSV ratio	ICA EDV cm/s
Normal	< 125	None	< 2.0	< 40
< 50%	< 125	< 50%	< 2.0	< 40
50%–69%	125–230	≥ 50%	2.0–4.0	40–100
≥ 70% to near occlusion	> 230	≥ 50%	> 4.0	> 100
Near occlusion	High, low, or undetectable	Visible	Variable	Variable
Total occlusion	Undetectable	Visible, no detectable lumen	N/A	N/A

(CCA: Common carotid artery; EDV: End-diastolic velocity; ICA: Internal carotid artery; PSV: Peak systolic velocity; ICA/CCA PSV ratio: Internal carotid artery to common carotid artery peak systolic velocity ratio).

A <50% ICA stenosis is diagnosed when ICA PSV is < 125 cm/s and plaque or intimal thickening is visible in the 2D gray-scale image. Additional criteria include ICA/CCA PSV ratio < 2.0 and ICA EDV < 40 cm/s. While a <50% diameter reduction may or may not cause a slight increase in the PSV, disturbed flow may become evident by color flow mapping or by increased Doppler spectral broadening, especially in the presence of eccentric plaques.

The authors do not recommend subcategorizing stenosis of <50% because this is likely to result in inaccuracy; however, the presence, location, and characteristics of ICA plaque should be described (Figs 33.20 and 33.21).

A 50 to 69% ICA stenosis is diagnosed when ICA PSV is 125 to 230 cm/s, and plaque is visible in the gray-scale images. Additional criteria include ICA/CCA PSV ratio of 2.0 to 4.0 and ICA EDV of 40 to 100 cm/s (Figs 33.22A to D and Movie clips 33.8 and 33.9).

A >70% ICA stenosis but less than near occlusion of the ICA is diagnosed when the ICA PSV is > 230 cm/s, and visible plaque and luminal narrowing are seen on gray-scale and color Doppler ultrasound. This threshold is quite sensitive, and incrementally higher values are correlated with more severe degrees of stenosis. Additional criteria for stenosis > 70% include ICA/CCA PSV ratio > 4 and ICA EDV > 100 cm/s. While the EDV threshold value is very suggestive of lesions > 70%, this parameter is not very sensitive because EDV varies with the heart rate and other systemic factors (Figs 33.23A to E and Movie clips 33.10 to 33.13).

As the degree of luminal narrowing increases, the increase in the intrastenotic flow velocity becomes the most important direct criterion for diagnosing a flow-limiting lesion. The ICA/CCA ratio and the EDV velocity increase as well. However, as the lesion progresses in severity, the resistance through the tight stenosis greatly affects the blood flow, causing a paradoxical low flow velocity (“string sign”).

This corresponds to the critical Grade III–IV stenosis in the Spencer’s curve, wherein significant decreases in the flow velocity and blood flow volume occur with >80% diameter stenosis (or more than 95% in cross-sectional area stenosis).⁴⁸

In cases of near occlusion of the ICA, the diagnostic velocity parameters may not apply, and velocities may be high, low, or undetectable. This diagnosis is therefore established primarily by demonstrating a markedly narrowed lumen with color or power Doppler ultrasound.

Total occlusion of the ICA should be suspected when there is no detectable patent lumen on gray-scale ultrasound and no flow with spectral, power, or color Doppler modalities. MRA, CTA, or conventional angiography may be used for confirmation in this setting.

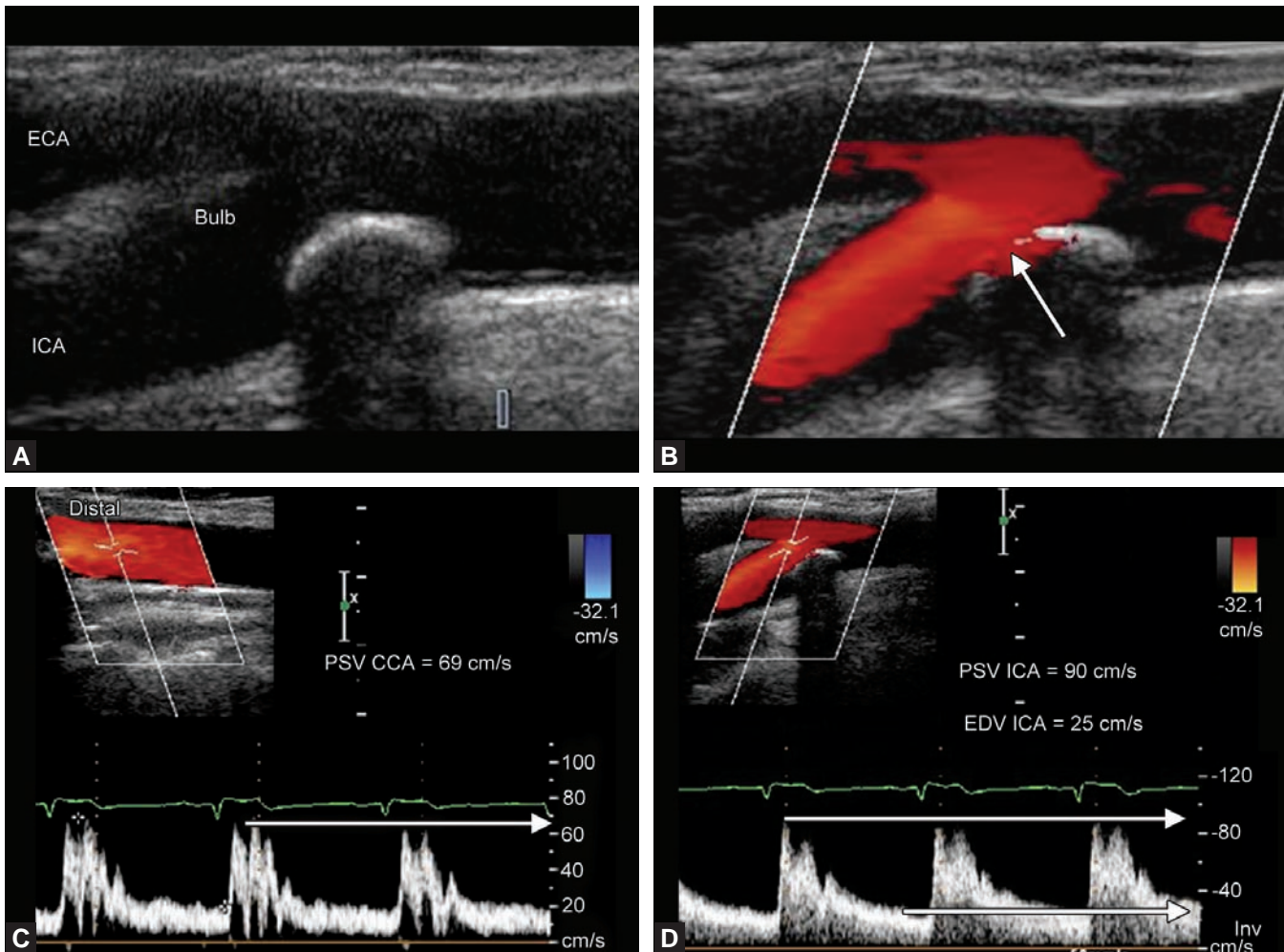
Validation of the 2003 Carotid Duplex SRU Consensus Criteria

During a 3-year period, AbuRahma et al analyzed 376 carotid arteries, for which both duplex examinations and digital angiography were available. Duplex scans were interpreted in accordance with the 2003 SRU Consensus Criteria for carotid artery stenosis, and arteriographic evaluations were performed using the NASCET method.

The study found that the consensus criteria had a sensitivity (Sn) of 93%, a specificity (Sp) of 68%, and an overall accuracy (OA) of 85% for detecting an angiographic stenosis in the range of 50–69%.

The authors concluded that the consensus criteria for diagnosing 50–69% stenosis could be significantly improved by using an ICA PSV of 140–230 cm/s (instead of 125–230 cm/s), which would have provided a Sn of 94%, a Sp of 92%, and an OA of 92%.

The consensus criteria performed well for stenosis ≥ 70%, with a Sn of 99%, a Sp of 86%, and an OA of



Figs 33.20A to D: Carotid bulb plaque with <50% stenosis. (A) The gray-scale image shows a calcified plaque with significant acoustic shadowing in the posterior wall of the carotid bulb; In (B) does not seem to have significant flow acceleration (white arrow) at this level; (C) and (D) Spectral Doppler shows the peak systolic velocity in the distal CCA is 69 cm/s; the peak systolic velocity in the ICA at the site of the plaque is 90 cm/s. The internal carotid artery/common carotid artery (ICA/CCA) ratio is therefore 1.3, and the end diastolic velocity of the ICA is 25 cm/s. These correspond to plaque in the carotid bulb with <50% of diameter stenosis by the consensus criteria. (CCA: Common carotid artery; ECA: External carotid artery; ICA: Internal carotid artery).

95%. The addition of the ICA EDV values or the ICA/CAA ratios did not produce significant improvement in the OA.⁴⁹

Near Occlusion versus Total Internal Carotid Artery Occlusion

The distinction between near occlusion and total occlusion of the ICA is very important because of the prognostic implications of the near occluded vessel for potential revascularization.

A severe stenotic lesion (defined by NASCET criteria as luminal narrowing in the 80–99% range) will present as an irregular, elongated, narrow-lumen lesion characterized by a so-called “string sign” or “trickle flow” in the color flow display. According to Spencer’s curve, flow velocity begins to decrease significantly beyond 80% diameter reduction, so such lesions will typically demonstrate low velocities. Their visualization may be enhanced by decreasing the color scale (Nyquist limit) and wall filter, increasing color gain, and increasing pulsed wave Doppler gain to optimize

the spectral tracing. The use of power Doppler or power angio may also be helpful to search for trickle flow.⁵⁰

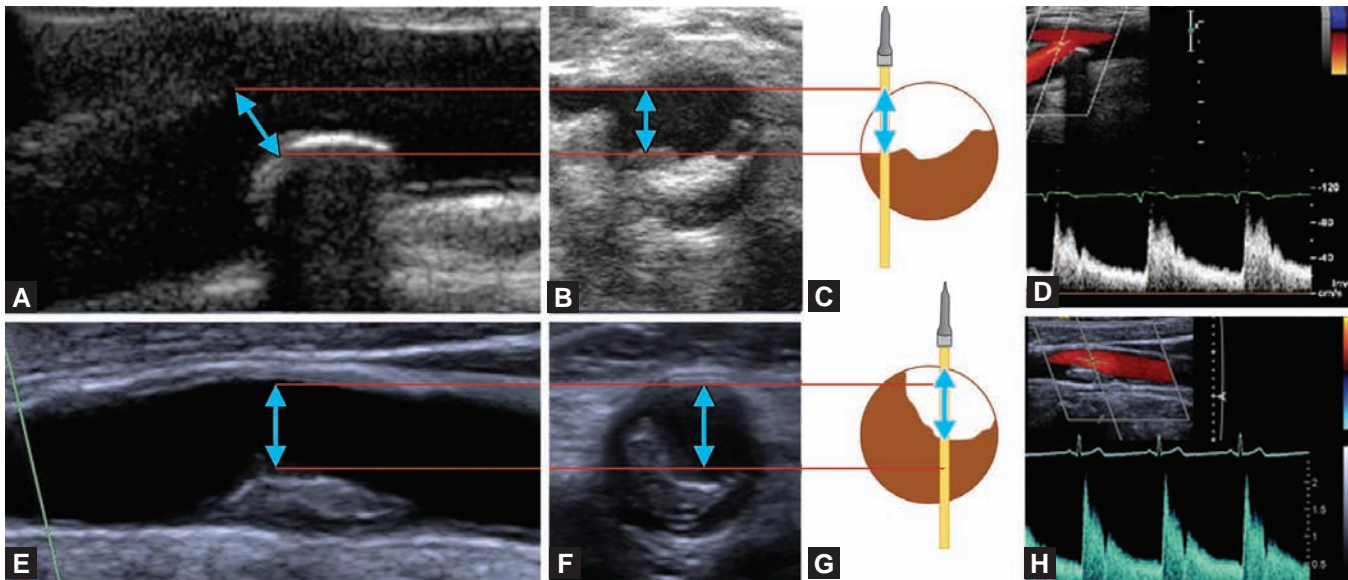
Other ultrasound findings in near occlusion of the ICA are:^{42,51}

- A decreased EDV of the CCA;
- “Internalization” of the ECA (high systolic velocity and increased diastolic flow) usually accompanied by ophthalmic artery flow reversal; and

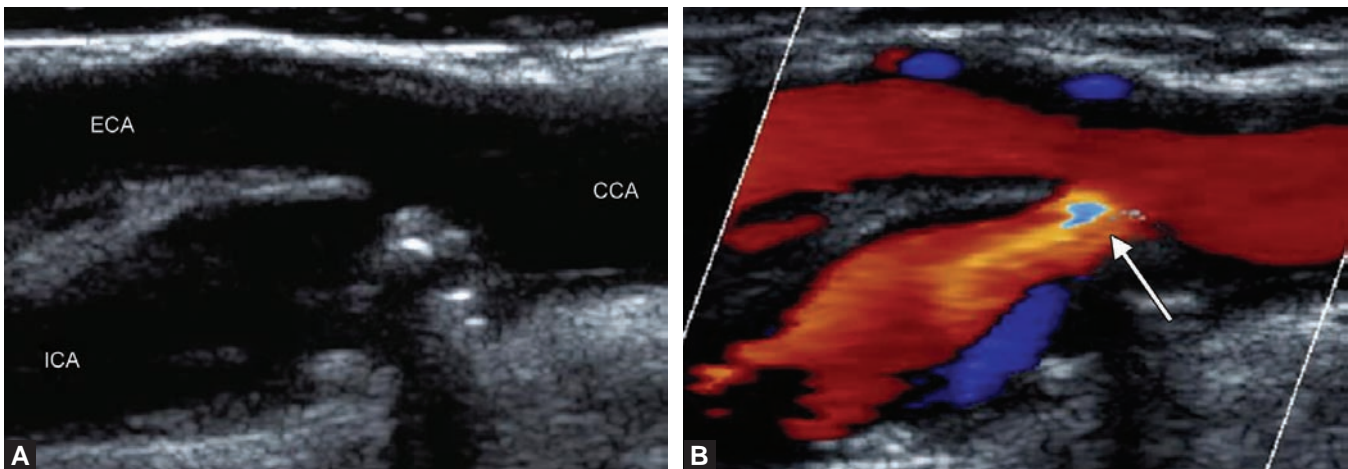
Increased velocity of the contralateral ICA (a possible consequence of increased collateral flow).

Ultimately, ultrasound contrast agents may prove helpful in improving diagnostic accuracy, in cases in which patency of the artery can not be established in spite of adequate image optimization, or in which significant doubts persists regarding identification of the trickle flow.

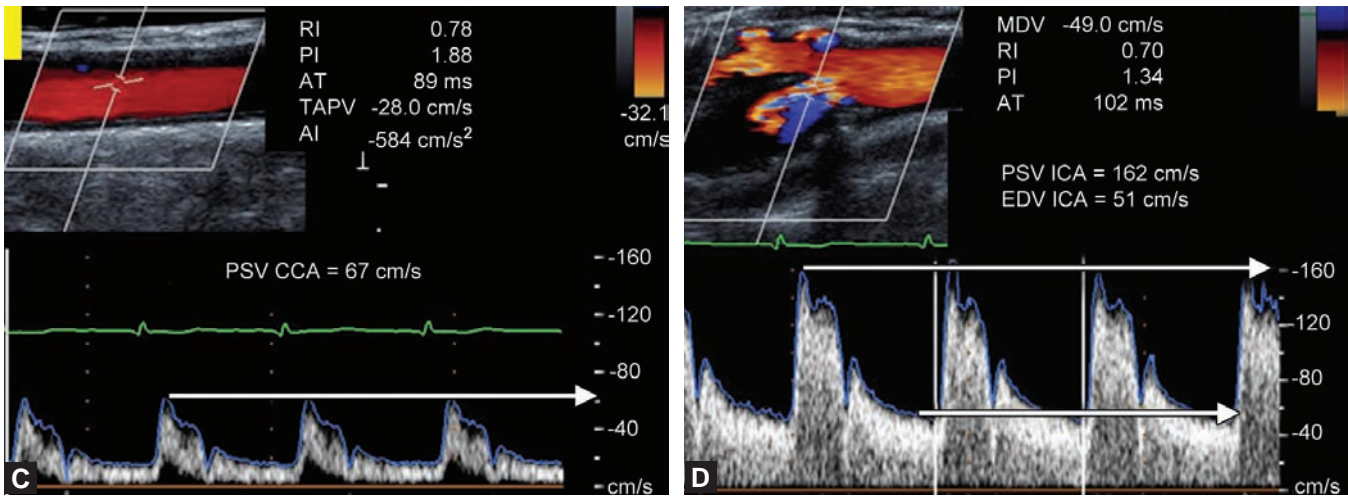
When an ICA is imaged in its usual anatomical location with no detectable color flow or spectral Doppler



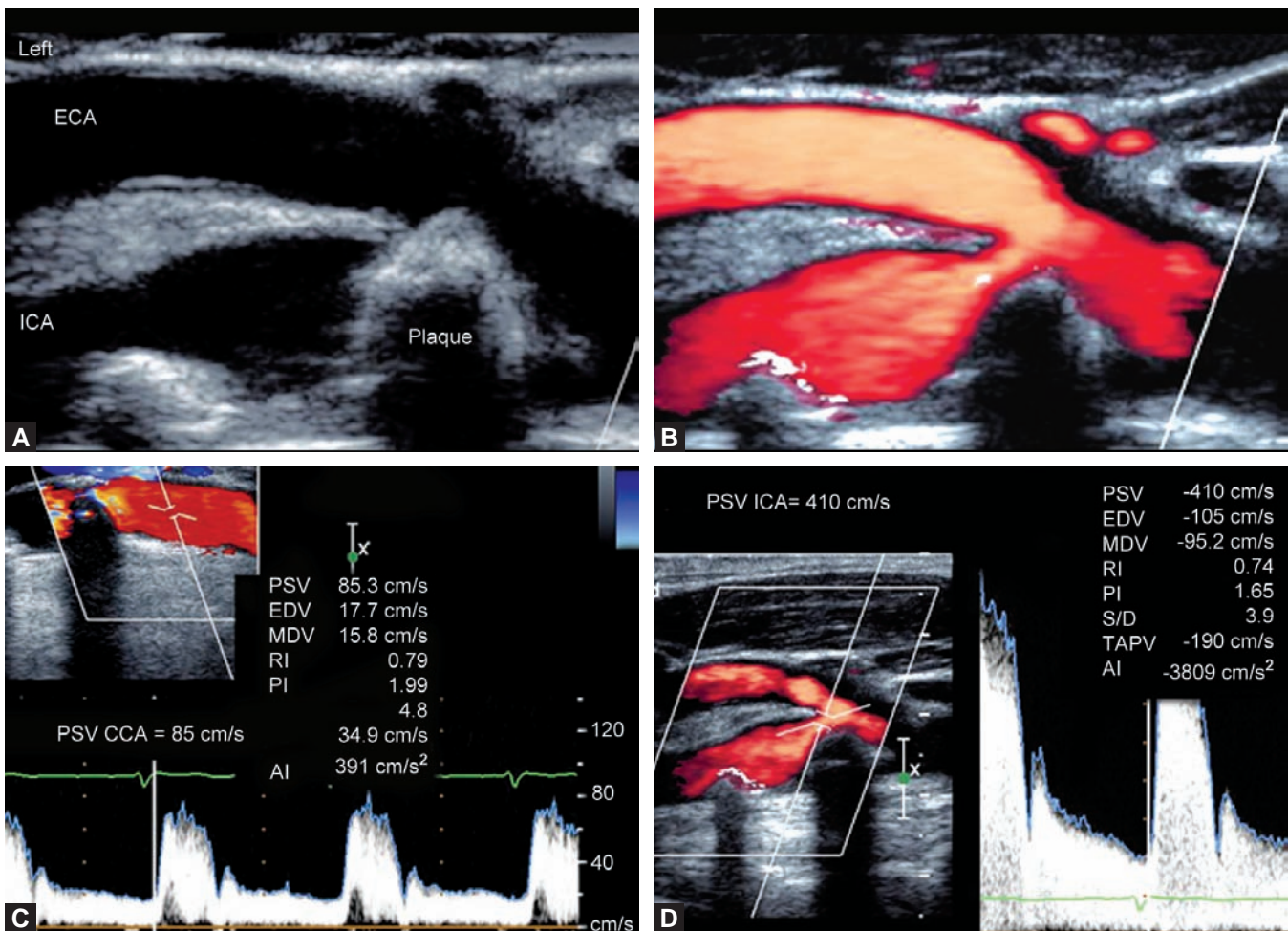
Figs 33.21A to F: Carotid plaque: longitudinal versus transverse view. (A) This carotid plaque (which corresponds to example in Figure 33.20), shows a small residual lumen in the bulb; however, in the transverse view in Figure B, the residual area is large and does not represent significant luminal narrowing. The eccentricity of the plaque illustrated in the diagram of Figure C, and the longitudinal scan of the carotid bulb clearly through the periphery of the artery gives the appearance of a small residual lumen. The velocities exhibited in Figure D are within normal limits. In (E to H) is shown the opposite situation. There is a predominantly echolucent plaque (Type 2) in Figure E with apparently no significant diameter reduction. The corresponding transverse scan in Figure F shows that the residual luminal area is small; and this discrepancy is related to the eccentricity of the plaque, and the longitudinal scan traversing through the largest residual diameter. Figure H shows increase in velocities consistent with moderate 50–69% stenosis. Therefore, it is extremely important to evaluate any lesion in both longitudinal and transverse views to adequately assess the degree of luminal narrowing.



Figs 33.22A and B



Figs 33.22A to D: Carotid bulb plaque with 50–69% stenosis. (A) Gray-scale image shows a large predominantly calcified plaque in the posterior wall of the carotid bulb, with significant flow acceleration (white arrow) demonstrated in (B) and in Movie clips 33.8 and 33.9. (C) and (D) The duplex study exhibits a peak systolic velocity in the CCA of 67 cm/s, and a peak systolic velocity in the ICA of 162 cm/s. The internal carotid artery/common carotid artery (ICA/CCA) ratio is 2.4 (> 2.0), and the end diastolic velocity in the ICA is 51 cm/s. These are consistent with moderate, 50–69% stenosis in the carotid bulb by the consensus criteria. (CCA: Common carotid artery; ECA: External carotid artery; EDV: End-diastolic velocity; ICA: Internal carotid artery; PSV: Peak systolic velocity).



Figs 33.23A to D:



Figs 33.23A to E: Carotid plaque with >70% stenosis. (A) There is a large, heavily calcified plaque in the posterior wall of the carotid bulb, right at the origin of the ICA. Movie clips 33.10 and 33.11 demonstrate significant luminal reduction and high aliasing flow during both systole and diastole, indicating high velocities at the stenosis during the entire cardiac cycle. There is also evident poststenotic turbulent flow. Movie clip 33.12 is a transverse view of the carotid bulb showing similar the heavily calcified plaque and the high velocity flow across the residual lumen; (B) The Power Angio mode enhances the flow across the stenosis and in the remaining ICA, which matches exactly to the three-dimensional computed tomography angiography (3D CTA) reconstruction shown in Figure E. Movie clip 33.13 corresponds to this figure. (C and D) The duplex study exhibits a peak systolic velocity in the distal CCA of 85 cm/s, and a peak systolic velocity in the ICA of 410 cm/s. The carotid artery/common carotid artery (ICA/CCA) ratio is 4.8 (>4.0), and the end diastolic velocity in the ICA is 105 cm/s. This data is consistent with severe >70% stenosis in the carotid bulb. (CCA: Common carotid artery; ECA: External carotid artery; EDV: End-diastolic velocity; ICA: Internal carotid artery; PSV: Peak systolic velocity).

signal, the vessel is said to have a total occlusion. While atherosclerosis is the most common cause of ICA occlusion, direct visualization of the plaque/thrombus complex within the vessel is not always an easy task, especially in chronic occlusions. Sometimes, however, there is a characteristic “to-and-fro” flow pattern at the point of occlusion known as “thud flow” on color Doppler and pulsed wave Doppler imaging. This finding is also called the “stump sign.”⁵⁰

Other duplex findings of total occlusion of the ICA are:⁵²

- “Externalization” of the CCA (in which vessels will exhibit similar Doppler tracings, with decreased diastolic flow in the CCA)

- Low systolic and diastolic velocities in the proximal CCA, lower in the neck.

- Increased diastolic flow in the ECA (as collaterals struggle to increase blood flow to the ipsilateral side).

- Increased flow velocities of the contralateral common and internal carotid arteries, similar to that in near occlusion.

Thus, optimization of all ultrasound parameters—color mapping velocity scale (PRF) and color gain, power Doppler, spectral Doppler thresholds, and wall filter—is paramount for the correct diagnosis of vessel occlusion (Figs 33.25A to D and Movie clips 33.14 and 33.15).

Effect of Significant Contralateral Disease on Internal Carotid Artery Stenosis Diagnosis

Several studies have shown that overestimation of the degree of ICA stenosis is likely in the presence of

contralateral high-grade carotid stenosis or occlusion, and this overestimation appears to be proportional to the severity of the contralateral disease.^{53,54}

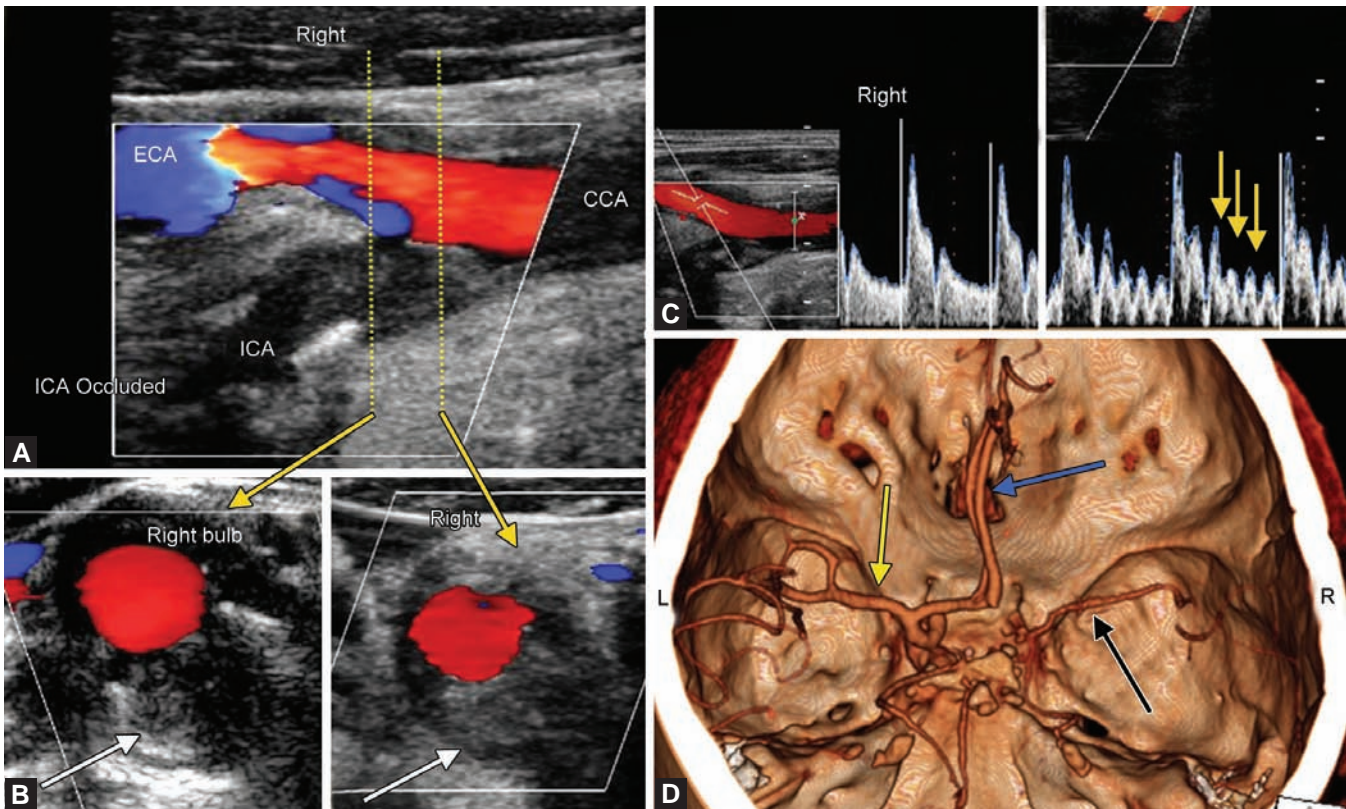
The increased velocities may be a consequence of increased collateral flow that is thought to represent a compensatory mechanism in the ipsilateral carotid system aimed at maintaining a stable cerebral circulation via the Circle of Willis.⁵⁴⁻⁵⁶

This phenomenon must be considered when applying established duplex velocity criteria to an ICA stenosis, as high velocities may be misconstrued as reflecting a higher degree of stenosis than is actually the case.

Assessment after Carotid Artery Endarterectomy and Stenting

The traditional standard of care in treating cervical carotid artery occlusive disease has been CEA, a procedure initially described in the 1950s by Scott, DeBakey, and Cooley. In 1991, landmark NASCET demonstrated a reduction in stroke and death rates at 2 years from 26% to 9% after endarterectomy. Since then, several other studies have suggested the superiority of the surgical approach to medical therapy for stenosis > 70%.

In the 1980s, angioplasty was pioneered for cervical carotid artery disease treatment, and the subsequent introduction of stent technology advanced nonsurgical interventional management of carotid artery disease. At present, there are two randomized clinical trials and six registries evaluating the safety and efficacy of carotid artery stenting (CAS).⁵⁷ Recently, the CREST trial showed that stenting and endarterectomy result in similar rates of the primary composite outcome (stroke, myocardial



Figs 33.24A to D: Occlusion of the ICA. (A) The color duplex image of the right carotid bifurcation demonstrates a large heterogeneous plaque filling the entire carotid bulb. There is no flow across the ICA, which is occluded. Movie clips 33.14 and 33.15 correspond to this figure; (B) Shows two cross-sectional views of the bifurcation demonstrating patency of the ECA, and the occlusion of the ICA (white arrows); (C) The ECA has increased compensatory flow velocity (“internalization of the ECA”). The temporal tap helps to confirm its identity and patency. The yellow arrows indicate the fluctuations in the baseline tracing of the ECA; (D) The brain computed tomography angiography (CTA) in this patient shows total or near total occlusion of the right ICA. A diminutive segment of the right middle cerebral artery (black arrow) is filled via Circle of Willis collaterals, and the right anterior cerebral artery (blue arrow) is filled via the anterior communicating artery. The left middle cerebral artery (yellow arrow) is of normal caliber. (ECA: External carotid artery; ICA: Internal carotid artery).

infarction, and death) among men and women with either symptomatic or asymptomatic carotid stenosis.⁵⁸

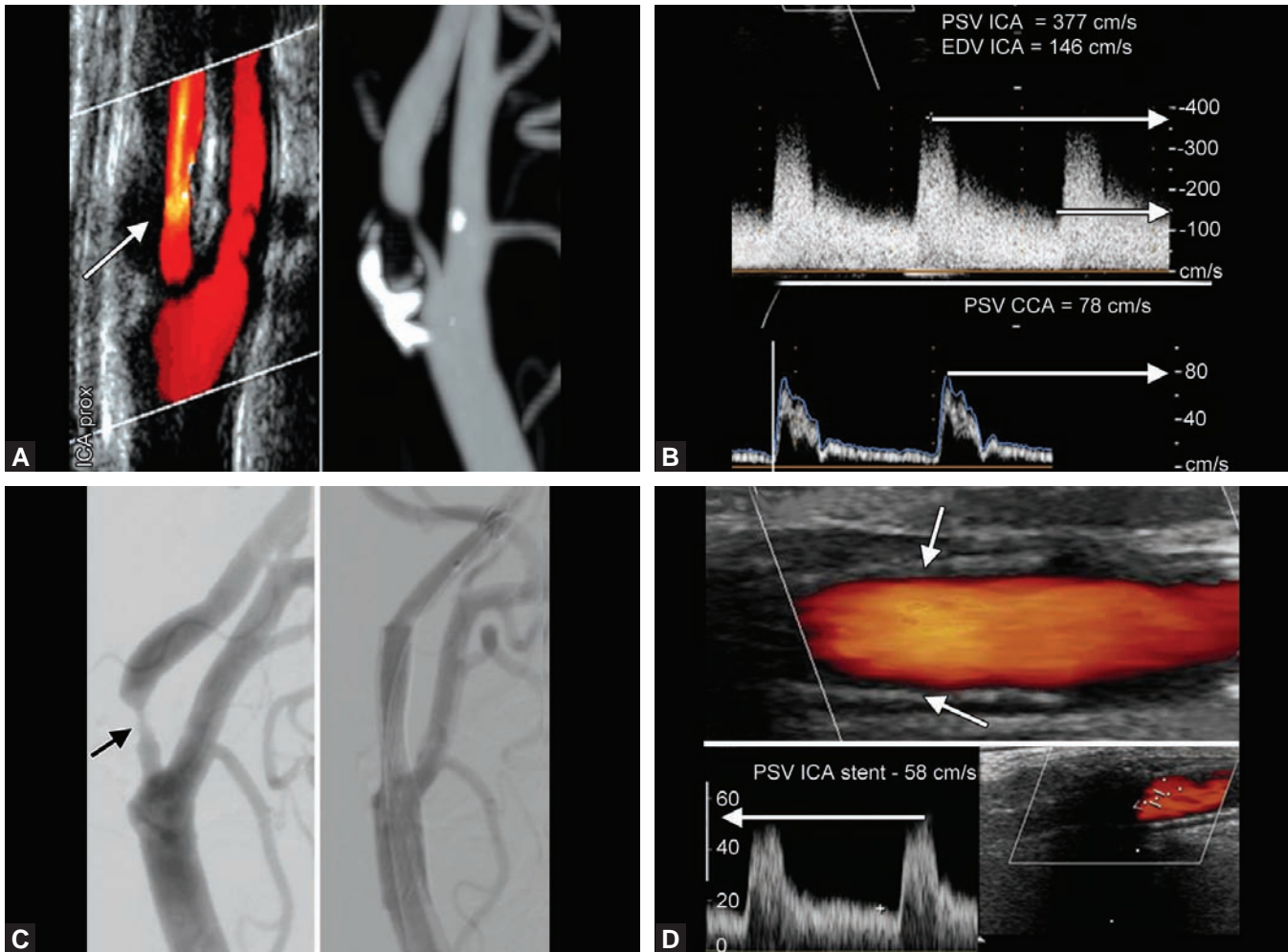
Duplex ultrasound is a reliable tool for surveillance post carotid artery endarterectomy and CAS, and criteria have been established for follow-up of both interventions. However, the timing and frequency of postintervention studies remains controversial. Several published reports have shown that most cases of restenosis occur within the first 2 years after CEA, and recommend an initial survey 6 months after surgery.⁵⁹⁻⁶¹

Following CEA, the intima-media layer at the surgical site is not seen. An “intimal step” at the proximal end is often seen, followed by bright reflectors in the anterior wall, which arise from the arteriotomy closure sutures.

Persistent flow disturbances and high velocities are usually the result of residual plaque and stenosis, which may be attributable to technically inadequate surgery that may have been prevented with placement of a synthetic or vein patch.

Restenosis at the surgical site within the first year is usually due to neointimal proliferation (overgrowth of smooth muscle and fibrous tissue in place of the striped intima-media following carotid intervention). In contrast, recurrence seen 3 years after CEA is usually due to the uninterrupted process of atherosclerosis.

Duplex ultrasonography is the standard technique for surveillance after CEA. In 2011, AbuRahma reported follow-up in 200 patients who had undergone CEA



Figs 33.25A to D: Carotid stenting. (A) Severe left ICA stenosis confirmed by CT angiography. The white arrow indicated the large plaque in the carotid bulb with small residual lumen. Movie clips 33.16 and 33.17 correspond to this figure; (B) Spectral velocity analysis shows the increased peak systolic and end-diastolic velocities in the ICA, with a carotid artery/common carotid artery (ICA/CCA) ratio of 4.8, consistent with severe >70% stenosis in the left carotid bulb; (C) The patient underwent angiography and carotid stenting with adequate lumen postintervention. Movie clip 33.18 shows the significant lesion in the left carotid bulb, and Movie clip 33.19 exhibits adequate residual lumen after stent deployment. (ICA: Internal carotid artery). 📺

with patching during a recent 2-year period. PSVs, EDV, and ICA/CCA ratios were correlated with angiography (ICA PSVs of ≥ 130 cm/s underwent carotid CTA and/or conventional carotid arteriograms to confirm the presence of post-CEA stenosis). The findings were:⁶²

- An ICA PSV > 213 cm/s optimally detected restenosis $\geq 50\%$ with a Sn of 99%, Sp of 100%, and OA of 99%.
An ICA EDV > 60 cm/s had a Sn, Sp, and OA of 93, 97, and 93%, respectively for detecting $\geq 50\%$ restenosis.
A PSV ICA/CCA ratio > 2.3 optimally detected restenosis of $\geq 50\%$.

- An ICA PSV > 274 cm/s was optimal for identifying $\geq 80\%$ restenosis with a Sn of 100%, Sp of 91%, and OA of 100%.

An ICA EDV > 94 cm/s had a Sn, Sp, and OA of 98, 100, and 98%, respectively for detecting $\geq 80\%$ restenosis.

A PSV ICA/CCA ratio > 3.4 was best for identifying restenosis $\geq 80\%$.

It must be noted that the placement of a stent in a carotid artery alters the mechanical properties of the vessel, producing higher velocities in the absence of residual stenosis or technical error. Because the reduced

compliance of a stented carotid artery may produce falsely elevated velocities relative to the native nonstented carotid artery, established ultrasound criteria for ICA stenosis are not appropriate for assessing restenosis after CAS.⁶³

The incidence of carotid restenosis may vary widely depending on the definition of restenosis and the method used to calculate the degree of stenosis. While several groups have proposed restenosis criteria, to date there is no consensus regarding what constitutes significant restenosis.

AbuRahma et al have confirmed the need for revised velocity criteria in stented carotid arteries. They reported on 144 patients who had undergone CAS as part of clinical trials. Follow-up consisted of carotid duplex ultrasound immediately after and 1 month after stenting, as well as every 6 months thereafter. Patients whose ICA PSVs were > 130 cm/s underwent carotid computed tomography (CT) or angiography to corroborate the presence of stenosis.

In this study, the PSVs, EDVs, and ICA/CCA ratios were recorded, and ROC analysis was used to determine the optimal velocity criteria for the diagnosis of angiographic in-stent restenosis of $\geq 30\%$, $\geq 50\%$, and $\geq 80\%$.⁶⁴

- To detect a stenosis of at least 30%, an ICA PSV of > 154 cm/s was optimal with a Sn of 99%, Sp of 89%, and OA of 96%.

An ICA EDV of 42 cm/s had a Sn, Sp, and OA of 86, 62, and 80%, respectively.

An ICA/CCA ratio of 1.5 was optimal.

- To identify a stenosis > 50%, an ICA PSV of > 224 cm/s was optimal with a Sn of 99%, Sp of 90%, and OA of 98%.

An ICA EDV of 88 cm/s had Sn, Sp, and OA of 96, 100, and 96%, respectively.

An ICA/CCA ratio of 3.5 was optimal.

- To diagnose a >80% stenosis, an ICA PSV of > 325 cm/s was optimal with a Sn of 100%, Sp of 99%, and OA of 99%.

An ICA EDV of 119 cm/s had Sn, Sp, and OA of 99, 100, and 99%, respectively.

An ICA/CCA ratio of 4.5 was optimal.

For all strata, the PSV of the stented artery was a better predictor of in-stent restenosis than the end-diastolic velocity or ICA/CCA ratio.

In 2008, Lal et al reported similar findings after reviewing 255 CAS procedures.

Available for analysis were 189 pairs of duplex ultrasound and either carotid angiography (29) or CT angiogram (99), during a median follow up of 4.6 years post-stenting.⁶⁵

Residual stenosis after CAS was defined as $\geq 20\%$ luminal reduction, the presence of in-stent restenosis was defined as $\geq 50\%$ luminal reduction, and hemodynamically significant high-grade in-stent restenosis was defined as $\geq 80\%$ luminal reduction.

ROC analysis demonstrated the following optimal threshold criteria:

- For residual stenosis > 20%, PSV > 150 cm/s, and ICA/CCA ratio > 2.2;
- For in-stent restenosis > 50%, PSV > 220 cm/s, and ICA/CCA ratio > 2.7; and,
- For in-stent restenosis > 80%, PSV 340 cm/s, and ICA/CCA ratio > 4.2.

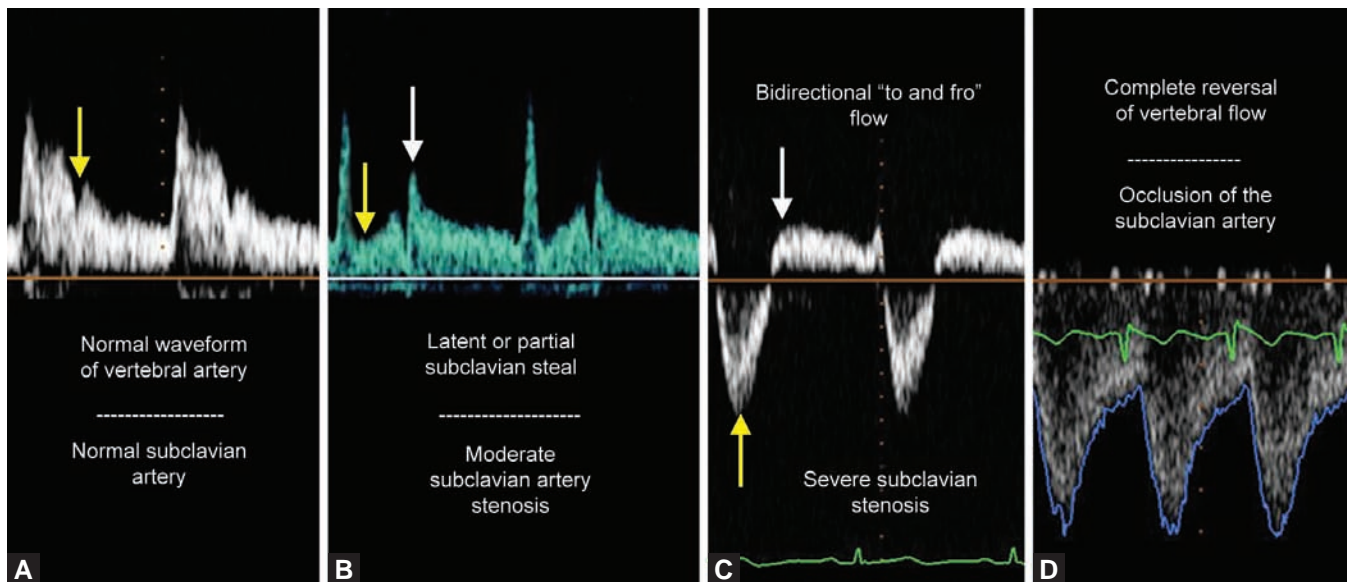
While both types of studies have limitations, these criteria are guidelines that may suggest the need for additional imaging when in-stent restenosis is suspected.

With the exponential rise in carotid stenting, intrastent restenosis is expected to become increasingly prevalent, and these patients will require close monitoring and ultrasound follow-up. Until new standardized duplex ultrasound criteria for CAS are established, follow-up velocities must be compared with earlier results after stenting. Persistent or recurrent elevation of PSVs may indicate progressive in-stent carotid restenosis and should warrant further investigation and appropriate clinical management.^{64,65}

Furthermore, because variants in the observed velocities may result from biomechanical alterations in the stented artery, it is possible that future modifications in stent composition and design may result in different velocity profiles. Whether or not these changes will be important enough to merit further revisions in the velocity criteria thresholds remains unknown⁶⁵ (Figs 33.26A to D and Movie clips 33.16 to 33.19).

Assessment of the Vertebral Arteries

The VAs provide approximately 20% of the total cerebral blood flow, and the vertebrobasilar system is not an uncommon site for acute ischemic events. However, the understanding of the mechanism of ischemia in the posterior circulation is less developed and there are fewer studies validating the diagnostic criteria for significant vertebrobasilar lesions than there are confirming the diagnostic criteria for carotid disease.⁶⁶ Nonetheless, Doppler interrogation of the proximal SAs and the extracranial portion of the VAs are integral parts of the cervical artery duplex ultrasound study and not infrequently a source of interesting hemodynamic findings.



Figs 33.26A to D: Vertebral artery and subclavian stenosis. (A) Normal vertebral artery spectral Doppler waveform: sharp systolic upstroke followed by forward diastolic flow. There is no evidence for significant stenosis in the proximal subclavian artery (or innominate artery in the right side); (B) Latent or partial subclavian steal. The vertebral Doppler waveform shows an early, rapid deceleration or “systolic dip” (yellow arrow), followed by a second more rounded diastolic forward flow (white arrow). This corresponds to a moderate degree of subclavian artery stenosis; (C) Bidirectional “to-and-fro” flow in the vertebral artery is seen with higher degree of stenosis in the ipsilateral subclavian artery. There is systolic reversal of flow in the vertebral artery (yellow arrow), followed by antegrade diastolic flow (white arrow); (D) Complete retrograde flow in the vertebral artery is seen with complete occlusion or near-occlusion of the ipsilateral subclavian artery. 📺

As mentioned earlier, the VAs are frequently asymmetric. In 50% of patients the left VA is dominant, in 25% the right VA is larger, and in the remaining 25% the two vessels are codominant.

Examination should be performed in multiple planes, to accurately demonstrate patency and direction of the flow. Almost all atherosclerotic stenosis of the VA occurs at its origin, making it crucial to follow the artery lower in the neck.

A PSV > 100 cm/s usually suggests a $\geq 50\%$ stenosis. High-grade stenosis is diagnosed when there is a marked increase in PSV of >150 cm/s.

Since there is wide variation in flow volume across these vessels, and velocities through the VAs are affected by differences in caliber (some vessels even being hypoplastic), the diagnosis of stenosis may be challenging. This is often of limited clinical impact since collateralization from the spinal arteries and contralateral VA tend to protect against posterior circulation ischemic insult.⁶⁷

Of greater hemodynamic significance is the presence of subclavian steal syndrome—flow reversal in one of the VAs in the setting of significant stenosis or occlusion of the ipsilateral proximal SA.

With significant stenosis in the SA, the pressure in the arm distal to the stenosis becomes lower than the pressure in the vertebral system. During systole, flow proceeds retrograde in the VA into the distal SA. In diastole, the gradient across the lesion is low and the pressure in the distal SA increases. Antegrade flow in the VA follows, producing a characteristic bidirectional Doppler waveform.²⁰

Symptoms suggesting transient posterior circulation ischemia may be occur, but the subclavian steal phenomenon seldom leads to cerebrovascular events.⁶⁶

The severity of the subclavian steal syndrome varies with the degree of the occlusive process in the SA and the relative role of the VA in supplying collateral flow to the arm. Several waveforms have been described indicating different grades of subclavian steal:^{20,67–69}

- A latent or partial subclavian steal is characterized by antegrade flow with an early systolic “dip” in the vertebral Doppler waveform, followed by a second more rounded systolic peak, and subsequent forward diastolic flow. This so-called “bunny rabbit waveform” (because of its resemblance to the profile of a rabbit) generally corresponds to a SA of $\geq 50\%$ stenosis. A high velocity jet created by the proximal ipsilateral

SA lesion, leads to a pressure drop in the VA, and the resulting transient siphoning of flow from the contralateral VA, producing this sharp deceleration after the first systolic upstroke. A “retrograde” dip in midsystole indicates a more severe stenosis in the SA.

- With higher degrees of SA stenosis, there is greater deceleration of flow in the VA. This produces a characteristic bidirectional “to-and-fro” flow, with initial retrograde systolic flow toward the arm, and subsequent antegrade diastolic flow toward the brain. The alternating Doppler signal indicates a high-grade ipsilateral SA stenosis.
- Complete retrograde flow in the VA is seen when there is complete occlusion or near-occlusion of the ipsilateral proximal SA (Figs 33.26A to D).

Subclavian steal syndrome can be caused by a lesion in either SA. It is important to note, however, that on the right side, when there is a significant stenosis or near-occlusion in the innominate artery, a “parvus and tardus” Doppler waveform (diminished amplitude and rounding of the systolic peak with delayed or prolonged systolic acceleration) will be seen in the right CCA as well. The flow in the ipsilateral VA will exhibit either bidirectional or the parvus and tardus characteristics, depending on the state of the contralateral VA.

A significant stenosis in the origin of the left CCA will result in a dampened monophasic waveform in the cervical segment of the vessel, with a typical parvus and tardus spectral display.

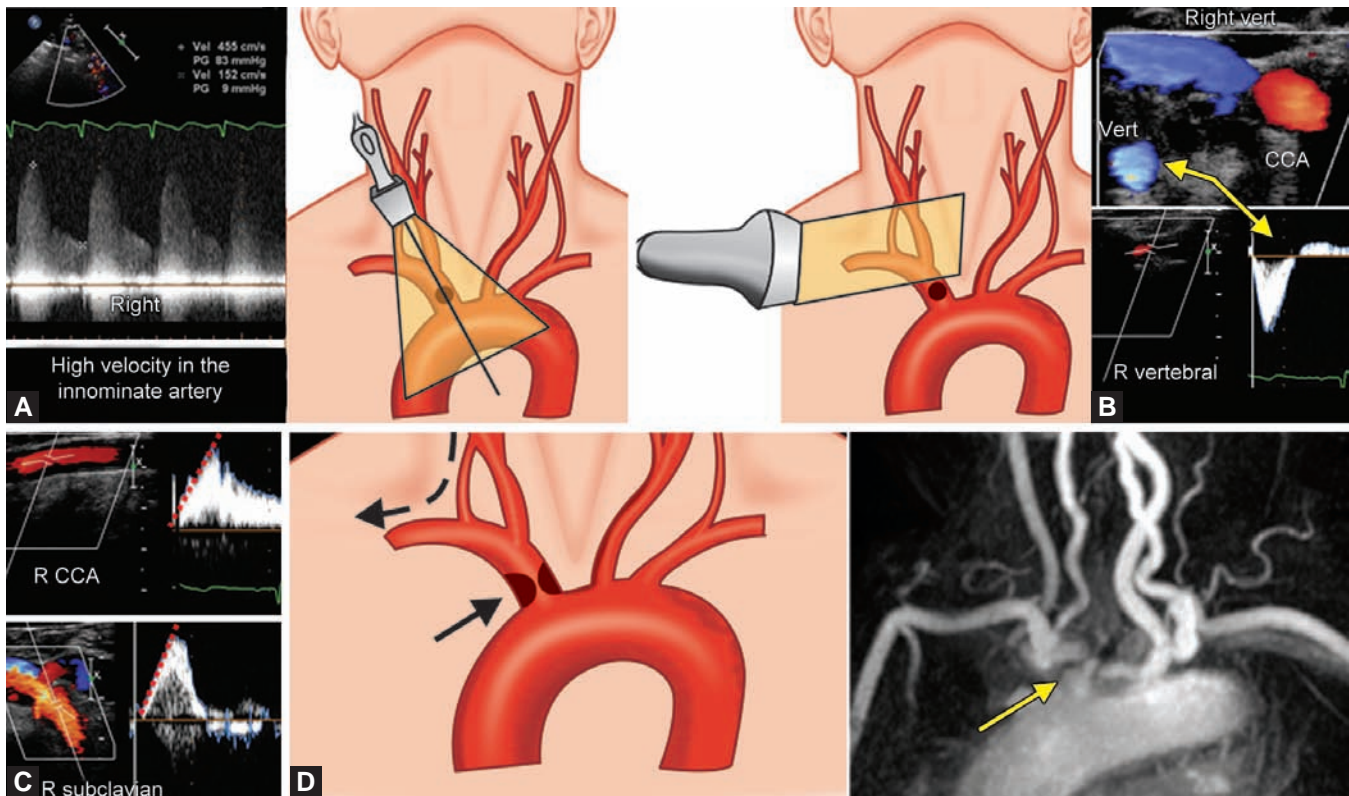
Any of the above findings during examination of the cervical arteries warrants thorough Doppler interrogation of the aortic arch vessels as described earlier in this chapter. In our experience, sonographers skilled in both adult echocardiography and vascular studies are better equipped to understand the significance of these hemodynamic riddles and to perform a more comprehensive examination of the entire supra-aortic circulation (Figs 33.27A to D).

Cardiac Pathology and Carotid Ultrasound Findings

During a routine carotid duplex study, atypical flow patterns not related to peripheral vascular disease may be encountered. Although, as echocardiographers, we have a thorough knowledge and understanding of cardiac disease entities, their hemodynamic alterations to flow in

the cervical arteries may lead to faulty interpretation of the peripheral arterial studies, if the association between the two is not established during the examination.

- *Aortic stenosis*: The flow pattern of a normal carotid artery usually has a fast upstroke with rapid acceleration time, a prominent dicrotic notch, and a diastolic wave. Mild to moderate aortic stenosis is unlikely to affect the carotid and subclavian velocity profiles. In patients with severe aortic stenosis, however, increased acceleration time, decreased peak velocity, delayed upstroke, and rounded waveforms may occur in the common carotid and SAs. When disease is not present in the cervical arteries, the presence of “parvus and tardus” changes in the cervical arteries should alert the examiner to the possibility of aortic stenosis. The velocity profile of the internal carotid arteries does not seem to be affected.⁷⁰
- *Aortic insufficiency*: Retrograde diastolic flow has been described in the ascending, descending, and abdominal aorta in patients with severe aortic regurgitation. Diastolic reversal of flow is always an abnormal finding in the carotid arteries, and it has been reported in patients with severe aortic insufficiency and with patent ductus arteriosus. The vessels most likely to exhibit diastolic reversal of flow are the proximal SAs, and to some extent, the common and external carotid arteries, presumably because they supply vascular beds with high resistance. In contrast, the ICA flow is directed to a low resistance bed, and while it may show decreased antegrade diastolic flow, it is unlikely to exhibit diastolic reversal of flow. The presence of a “bisferiens pulse” (two distinct systolic peaks) in the CCAs may also suggest significant aortic regurgitation. However, a similar Doppler pattern may be seen in the carotid arteries of patients with hypertrophic obstructive cardiomyopathy and significant left ventricular outflow tract gradients.⁷¹
- *Intra-aortic balloon pump*: An IABP will limit the Doppler evaluation of the carotid arteries. As the balloon inflates and deflates with each cardiac cycle (1:1 setting), it creates a second, typically higher peak that coincides with diastolic balloon counterpulsation. The disruption of blood flow by the balloon, thus precludes the use of standard velocities and waveforms in the assessment of carotid stenosis^{22,72} (Figs 33.28A to D).
- *Left Ventricular Assist Device (LVAD)*: LVADs are increasingly being implanted for heart failure



Figs 33.27A to D: Subclavian steal syndrome. This is part of the study performed in a 72-year-old man, referred for a transthoracic echocardiogram, to assess the degree of aortic stenosis after a significant murmur was heard during routine examination. The two-dimensional (2D), color flow, and Doppler evaluation of the aortic valve did not reveal significant pathology. (A) During color flow and Doppler interrogation of the aortic arch and great vessels, high velocity flow is found in the innominate artery; (B) The sonographer then proceeds to evaluate the right side cervical arteries. During a transverse scan of the neck, the CCA and the vertebral artery exhibit opposite flow direction (CCA in red and vertebral artery in blue) during systole. Indicated by the yellow arrows there is evidence for systolic reversal of flow in the right vertebral artery (bidirectional “to-and-fro” flow), consistent with subclavian steal syndrome; (C) The right CCA and the distal right subclavian artery exhibit characteristic “parvus and tardus” spectral Doppler tracings, which in fact strongly suggests the location of the lesion in the innominate artery (the innominate artery divides into the right common carotid and right subclavian arteries); (D) Magnetic resonance angiography of the aortic arch and great vessels confirm the presence of a severe stenosis in the innominate artery (yellow arrow). (CCA: Common carotid artery).

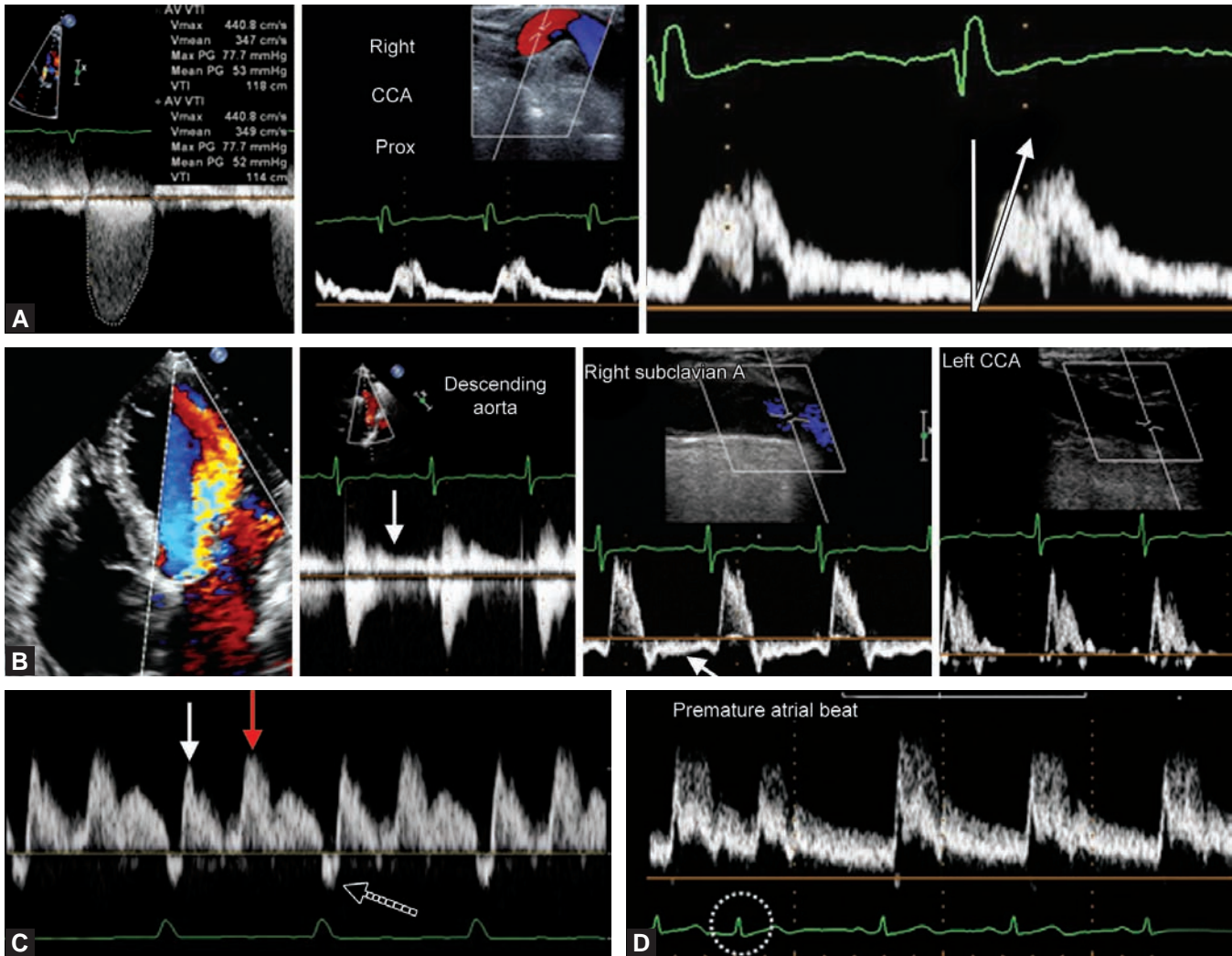
Courtesy: Illustration created by Melissa LoPresti and Robert Spencer, NYU).

refractory to medical therapy—as bridges to myocardial recovery, or cardiac transplantation, or as destination therapy for patients who are not candidates for heart transplant.

The HeartMate II is the device most frequently used in our institution. Doppler waveforms in the carotid and VAs resemble “parvus and tardus” flow, being characterized by monophasic flow with dampened PSV, round-shaped systolic peak, and prolonged acceleration.⁷³ The marked alteration in waveform morphology and velocities created by the device renders the diagnosis of stenosis impossible by velocity criteria. Sonographers should, therefore, emphasize the gray-scale features to elucidate the presence of carotid disease.

ULTRASOUND DIAGNOSIS OF FEMORAL ACCESS COMPLICATIONS

In the last decade, medicine has witnessed an exponential growth in percutaneous coronary, peripheral arterial, and now structural heart disease interventions, as well as cardiac electrophysiology procedures. The common femoral artery and vein continue to be the preferred and most commonly used access sites for the performance of these techniques. Although the use of arterial closure devices has increased the safety of vascular cannulation, femoral access-site complications remain a major cause of morbidity, patient discomfort, and prolonged length of hospital stay.



Figs 33.28A to D: Cardiac pathology and carotid Doppler findings. (A) In the absence of significant disease in the cervical arteries, the finding of “parvus and tardus” Doppler waveforms in several vascular territories in the neck suggests the possibility of severe aortic stenosis as cause of the altered tracings. Note the significant delay and round shape of the systolic upstroke, and the prolonged deceleration; (B) Patient with severe aortic regurgitation exhibits diastolic reversal of flow in the descending thoracic aorta and in the subclavian artery (white arrows). The common carotid artery may show cessation of the forward diastolic flow (as shown in this particular case in [B]) or reversal of flow; (C) Spectral Doppler tracing in a patient with an intra-aortic balloon pump. After the initial systolic upstroke (white arrow), there is a second, typically higher peak (red arrow) that coincides with diastolic balloon counterpulsation. There is a third, short, retrograde waveform, which coincides with balloon deflation (dotted arrow). A simultaneous electrocardiogram tracing helps to correlate events and differentiate from premature atrial or ventricular activity (D).

Duplex ultrasound has become the “gold standard” and first-line diagnostic imaging modality to assess for vascular access-site complications, particularly those using the femoral approach. It is important that physicians caring for patients returning from the catheterization laboratory be able to recognize the presentation and ultrasonographic features of the most common post-procedural complications, and be mindful of the different treatment options.

The overall incidence of vascular access-site complications ranges broadly from 0.7% to 9%. This wide variation is related to whether the procedures are purely diagnostic or include therapeutic interventions. Prolonged interventions, the use of larger sheath size, and the aggressive use of antiplatelet agents and anticoagulants, make hemostasis more difficult to achieve, and result in an increased incidence in complications at the puncture site.⁷⁴

Vascular complications can be divided into:⁷⁵

- Minor complications:
 - Minor bleeding
 - Ecchymosis
 - Stable small hematomas.
- Major complications:
 - Pseudoaneurysm
 - Arteriovenous (AV) fistulas
 - Large hematomas requiring transfusion
 - Retroperitoneal hematoma
 - Arterial dissection
 - Infection
 - Thrombosis
 - Limb ischemia.

Several patient and procedure-related risk factors may contribute to the development of complications at the femoral access site.⁷⁵⁻⁷⁷

- Patient-related risk factors:
 - Older age
 - Female gender
 - Obesity or low body weight
 - Peripheral vascular disease
 - Hypertension
 - Chronic renal failure
 - Low platelet count.
- Procedure-related risk factors:
 - High puncture site (above the inguinal ligament)
 - Low puncture site (below common femoral bifurcation)
 - Through-and-through puncture/multiple punctures
 - Prior catheterizations at the same site
 - Large sheath size
 - Concomitant venous sheath
 - Prolonged procedure time
 - Long indwelling sheath time
 - Use of antiplatelet therapy (ASA, clopidogrel, GPIIb/IIIa, etc.)
 - Use of anticoagulants
 - Inadequate postprocedure compression to achieve hemostasis
 - Premature ambulation.

Bleeding and hematoma are the most common complications of the transfemoral approach. They may occur during the intervention because of failed puncture of the artery, during sheath removal, or subacutely hours after the procedure.⁷⁷ Ecchymosis and small hematoma are common. They are often superficial, originate from the anterior aspect of the vessel, and generally resolve

spontaneously over a few weeks as the blood degrades and by-products are reabsorbed. However, persistent uncontrolled bleeding can lead to large hematomas with significant swelling and discomfort in the femoral region, and may take several weeks or months to resolve (Figs 33.29A to C and Movie clips 33.20-33.23).

Large hematomas can cause compression of the femoral or iliac veins leading to lower extremity edema or even deep venous thrombosis, and femoral nerve compression may result in muscle weakness.

Bleeding from a high arterial puncture above the inguinal ligament or a deep puncture after posterior transfixion of the artery may have catastrophic consequences if overlooked.

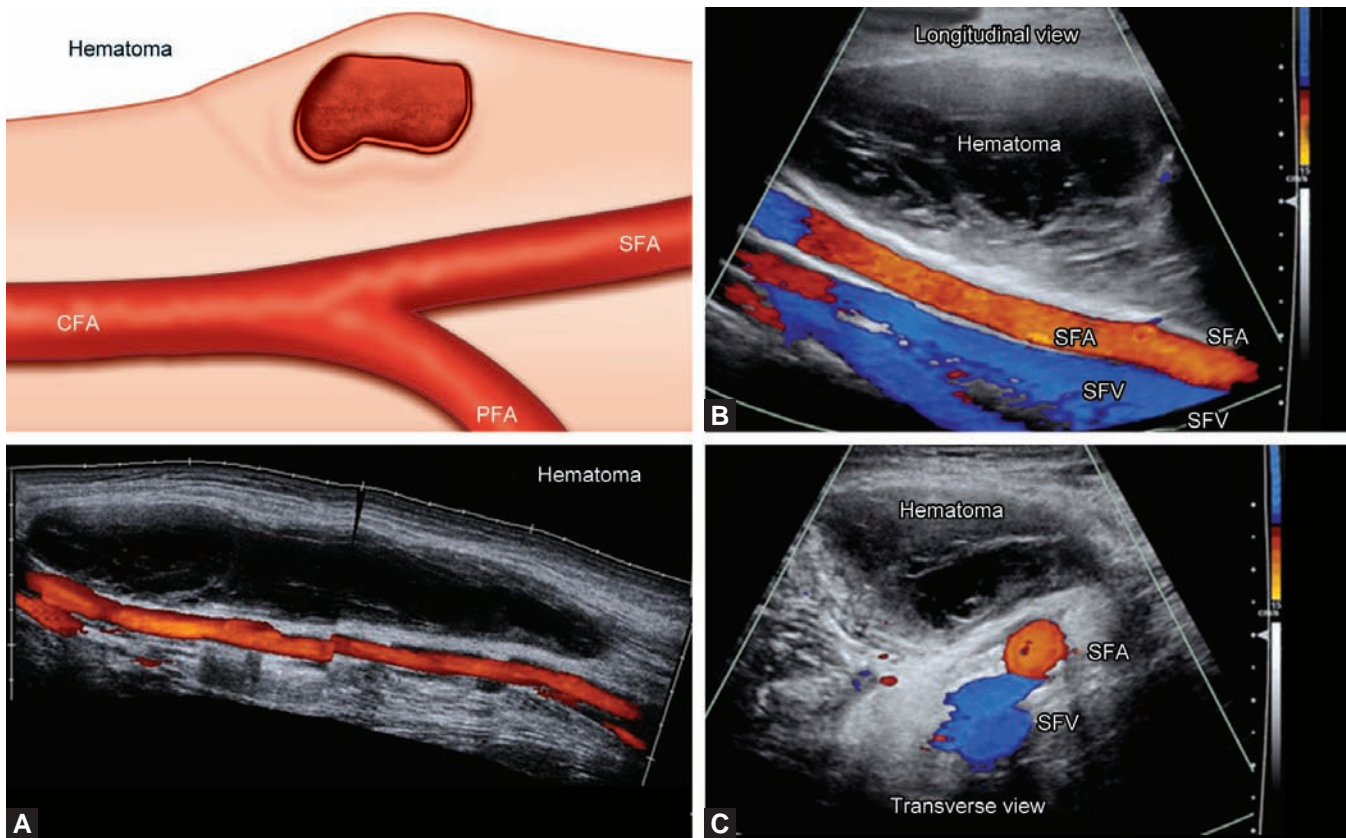
Retroperitoneal bleeding is a life-threatening complication that has been reported to occur in 0.12-0.44% of percutaneous interventions,⁷⁸ and should be suspected in any postcatheterization patient who develops ipsilateral flank, abdominal or back pain, profound hypotension, or a drop in hematocrit without a clear source. The retroperitoneal space can accommodate an enormous amount of blood before local signs become manifest or hemodynamic deterioration occurs.^{75,76}

A pseudoaneurysm is a collection of blood and thrombus encapsulated by the adjacent soft tissue that remains connected to the artery by way of a neck created by the needle track. The reported incidence of pseudoaneurysm is 0.5-1.5% after diagnostic catheterizations and 2.1-6% following interventional procedures. It has been found to be as high as 7.7% when duplex examinations are routinely performed after all procedures.⁷⁹⁻⁸²


Pseudoaneurysm usually originates at the site of femoral access and is associated with punctures below the bifurcation of the common femoral artery, difficult hemostasis due to lack of bony structures beneath the superficial and profunda arteries, and inadequate compression.

The clinical presentation is usually that of an enlarging painful mass in the groin area surrounded by extensive ecchymosis. On examination, there is typically a palpable, tender, pulsatile mass, with or without a systolic bruit, but the presenting signs vary. The presence of a palpable "thrill" or auscultation of a continuous bruit over the groin should raise concern for coexistent AV fistula.⁸³ Any clinical suspicion warrants further investigation with ultrasound.

Color duplex ultrasound is considered the modality of choice to establish the diagnosis of femoral pseudoaneurysm and is nearly 100% accurate. The Sn of



Figs 33.29A to C: (A) Hematoma after femoral artery access; (B and C) These large field of view images from a C6-2 MHz curvilinear transducer demonstrate normal superficial femoral artery and vein, with no connection to the hematoma (no residual tract). The hematoma is completely thrombosed. Movie clips 33.20 and 33.21 demonstrate normal common femoral artery and vein, with no evidence of AV fistula. Movie clips 33.22 and 33.23 demonstrate normal superficial femoral artery and vein in longitudinal and transverse scan, with no visible tract connecting with the thrombosed hematoma.

Courtesy: Illustration created by Melissa LoPresti and Robert Spencer, NYU). 

duplex ultrasound to identify pseudoaneurysm is 94% with a Sp of 97%.⁸⁴

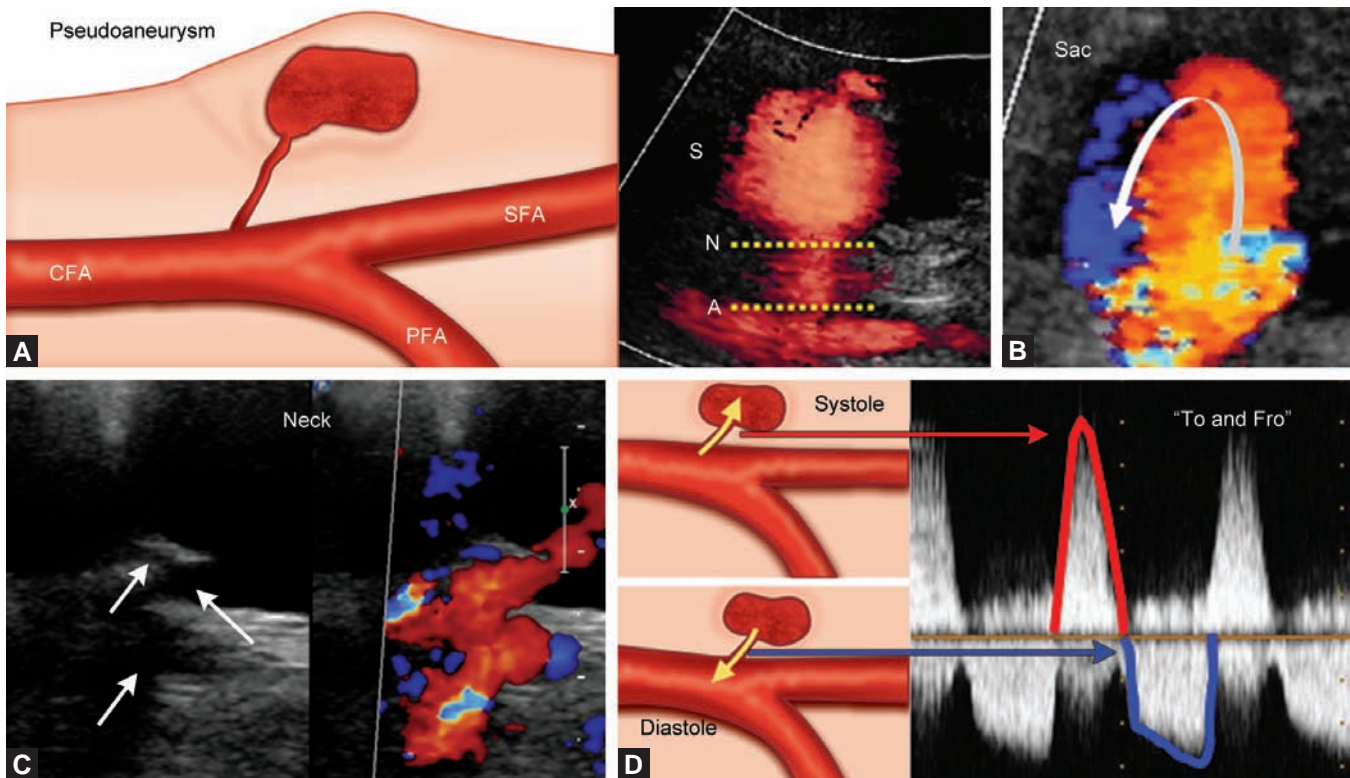
Typically, the patient is placed supine with the ipsilateral leg externally rotated to better expose the groin area. A 5–7 MHz linear array transducer may be used, but extensive soft tissue edema may limit resolution. A curved array probe with lower frequency is therefore preferable to improve penetration and create a larger field of view.⁸⁵

As with any other vascular structure, both longitudinal and transverse views of the external iliac and femoral arteries and veins should be obtained. We recommend starting exploration high in the external iliac territory and moving downward toward the proximal superficial and profunda femoral artery and veins. Adequate spectral Doppler samples of both arteries and veins should be obtained. Even when the presumptive diagnosis is pseudoaneurysm, the coexistence of other complications must be excluded.

The characteristic features of a pseudoaneurysm by duplex ultrasonography are best described as three main structures:^{83,85}

The false aneurysm sac—an irregular, occasionally multilobulated, vascularized cavity that usually measures 3–6 cm (but is sometimes larger), containing a swirling pattern of flow. The location of the cavity and presence of thrombus should be noted, and the size measured in at least two dimensions. It is not uncommon for more than one or two interconnected chambers to be seen.

The neck—an irregular, cylindrical tract that connects the cavity with the artery. A pathognomonic feature exhibited by the neck, when interrogated with pulsed wave Doppler, is a “to-and-fro” flow. This characteristic spectral Doppler pattern reflects the changes within the cardiac cycle: In systole, the pressure in the artery is higher than the pressure in the sac, directing the flow toward the false aneurysm cavity. In diastole, the pressure in the sac is



Figs 33.30A to D: Pseudoaneurysm after femoral artery access. (A) Duplex ultrasound with Power Angio show the three components of a pseudoaneurysm, (S) the aneurysmal sac, (N) the neck or needle tract, and (A) the feeding artery; (B) Shows the aneurysmal sac with typical swirling of flow. Movie clips 33.24 and 33.25 correspond to this figure; (C) These gray-scale and color flow images show an irregular tract that constitutes the neck of the pseudoaneurysm and (D) demonstrates the characteristic “to-and-fro” flow during Doppler interrogation: in systole, the pressure in the artery is higher than the pressure in the sac; therefore, the flow is toward the aneurysmal sac. During diastole, the flow is directed backward toward the artery. Movie clips 33.26 and 33.27 demonstrate the typical “to-and-fro” flow through an irregular neck created by the needle tract.

Courtesy: Illustration created by Melissa LoPresti and Robert Spencer, NYU. 

higher than the pressure in the feeding artery, so the flow empties from the cavity. The identification of such a high pulsatility tract makes the diagnosis of pseudoaneurysm a certainty. It is essential to record the length and the width of the neck, since both have therapeutic implications.⁸⁶

The feeding artery—usually the common femoral or superficial femoral artery. The disruption of all three layers of the artery happens more often in the anterior aspect of the vessel, but is not uncommon in cases of posterior transfixion of the artery for the tract to have a deeper trajectory. In such cases, the diagnosis of pseudoaneurysm may become more challenging. Careful attention should be paid to the depth of the field of view, so deep tracts and cavities are not overlooked. In cases in which access was difficult and multiple puncture attempts were required, more than one tract may be found (Figs 33.30A to D and Movie clips 33.24 to 33.27).

Small pseudoaneurysms (3 cm or less) in asymptomatic patients can be followed up with serial ultrasound examinations, as they usually spontaneously close within few weeks. Toursarkissian et al. followed up 286 lesions including 196 pseudoaneurysms, 81 AV fistulae, and 9 combined lesions. They reported spontaneous closure of the pseudoaneurysm in 86% of the patients who were selected for conservative management.⁸⁷ Several other small studies have shown similar results. In the literature, there are no specific duplex ultrasound findings described other than size < 3 cm, as valid predictor of spontaneous resolution.

Larger pseudoaneurysms (> 3 cm or expanding hematomas), combined lesions, or patients who are symptomatic or require chronic anticoagulation should be managed with a different strategy.

In 1991, Fellmeth et al described the use of ultrasound-guided compression—a nonsurgical approach for those patients who are not eligible to be managed conservatively.⁸⁸

The technique consists of the manual compression of the pseudoaneurysm by a physician or an experienced sonographer under direct ultrasound visualization. It is recommended the use of a 5 MHz curvilinear probe, which provides a wide and deep field of view, and facilitates the task of exerting continuous pressure.

Pressure to the cavity and the neck of the pseudoaneurysm should be applied for about 10–15 minute intervals, until the “to-and-fro” flow is completely stopped. Careful attention should be paid to ensure adequate flow in the femoral artery while preventing flow into the pseudoaneurysm; however, some degree of compression of the artery may be unavoidable. After completion of the first interval, the pressure is slowly released and blood flow into the lesion is reassessed. If there is persistent flow through the neck, the same procedure may be repeated once or twice until thrombosis of the neck and pseudoaneurysm is accomplished or it exceeds a discretionary failure time. In general, patients should be given analgesia or sedation before procedure to minimize the discomfort created by exerting pressure in the affected groin area.^{83,85,86}

The success rate for ultrasound-guided compression ranges from 60% to 90%, but in patients who are on anticoagulation therapy, complete resolution can be achieved only in 30–75% of the cases.^{89,90}

The most important predictors of successful treatment are the size of the pseudoaneurysm, and the length and width of the neck. Larger aneurysm sacs, and short and wide tracts have the least rate of success. A major disadvantage of ultrasound-guided compression is the time to achieve obliteration. It has been reported in compression times exceeding 1 hour⁸¹ (Figs 33.31A and B).

Another technique—ultrasound-guided thrombin injection—is a safe alternative to ultrasound-guided compression therapy, and it has been used frequently since first described by Cope and Zeit in 1986.⁹¹

A 0.1–0.3 mL saline dilution of 1000 U/mL bovine thrombin is slowly injected into the pseudoaneurysmal sac under direct ultrasound visualization. Thrombosis of the pseudoaneurysm cavity is achieved, usually, within 5–10 seconds after injection. Complete obliteration of the sac should be confirmed by color-flow Doppler, as well as patency of the femoral artery and vein. In general, an interventionalist or a vascular surgeon performs this

procedure. It is very important to position the needle tip just inside the sac, and as far as technically possible away from the neck, to avoid forcing thrombin into the tract and therefore into the femoral artery.⁸³ Embolization to the femoral artery following thrombin injection has been reported in <1%.

Ultrasound-guided thrombin injection has a higher technical success rate than ultrasound-guided compression. Complete obliteration of the sac is achieved in 91–100% in the first attempt, with a very low recurrence rate.⁸⁶ This approach is also very effective in patients who are on anticoagulation therapy.

Paulson et al reported a success rate of ultrasound-guided thrombin injection of 96% compared with 74% in the compression repair group. The average time for complete obliteration was 6 seconds for thrombin injection, compared with 41 minutes for compression.⁹²

Although most patients are good candidates for ultrasound-guided thrombin injection, there are contraindications to the technique that must be recognized.⁸⁵

- Infected pseudoaneurysm
- Ischemia of the overlying skin
- Distal limb ischemia
- Allergy to thrombin
- Short of absence of pseudoaneurysm neck
- Small cavity size ≤ 1 cm.

If any of these contraindications is present, surgical repair of the pseudoaneurysm should be considered the best treatment strategy.

The simultaneous puncture of the femoral artery and the vein can lead to the creation of an AV fistula.

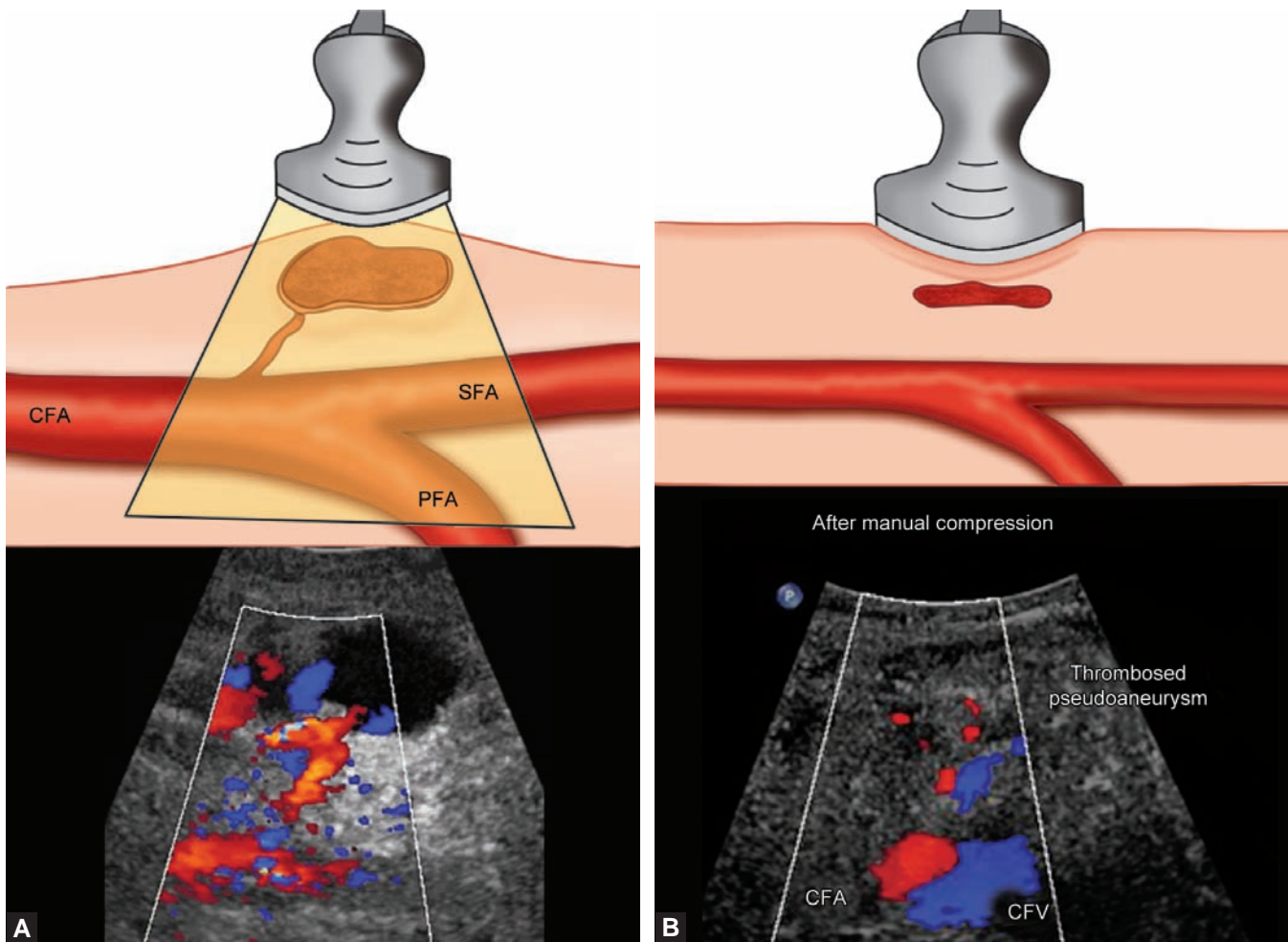
The incidence of AV fistula has been reported to be in the range of 0.2–2.1% after cardiac catheterization.⁷⁵

Risk factors that increase the risk of AV fistula are:

- Multiple punctures to obtain vascular access
- Overlying femoral artery and vein
- Lower puncture below the common femoral artery bifurcation
- Impaired clotting.

AV fistulas are often asymptomatic; however, patients may present with an ipsilateral edema due to venous congestion, arterial ischemia due to steal syndrome, and in large chronic fistulas high output heart failure has been reported. Auscultation may reveal a continuous bruit in the femoral area.

Duplex ultrasound examination demonstrates increased systolic and diastolic flow velocity in the common femoral artery with a very low resistance pattern.



Figs 33.31A and B: US-guided compression therapy of pseudoaneurysm. (A and B) show a successful ultrasound-guided compression of a femoral artery pseudoaneurysm. (CFV: Common femoral vein; CVA: Common femoral artery; PFA: Profunda femoral artery; SFA: Superficial femoral artery).

Courtesy: Illustration created by Melissa LoPresti and Robert Spencer, NYU).

The common femoral vein also exhibits increased flow with a typical “arterialization” of the spectral Doppler tracing, which is proof of the presence of a “shunt” between the artery and vein. The respiratory variations in the vein are significantly diminished. Doppler interrogation of the “shunt” will exhibit very high velocity.

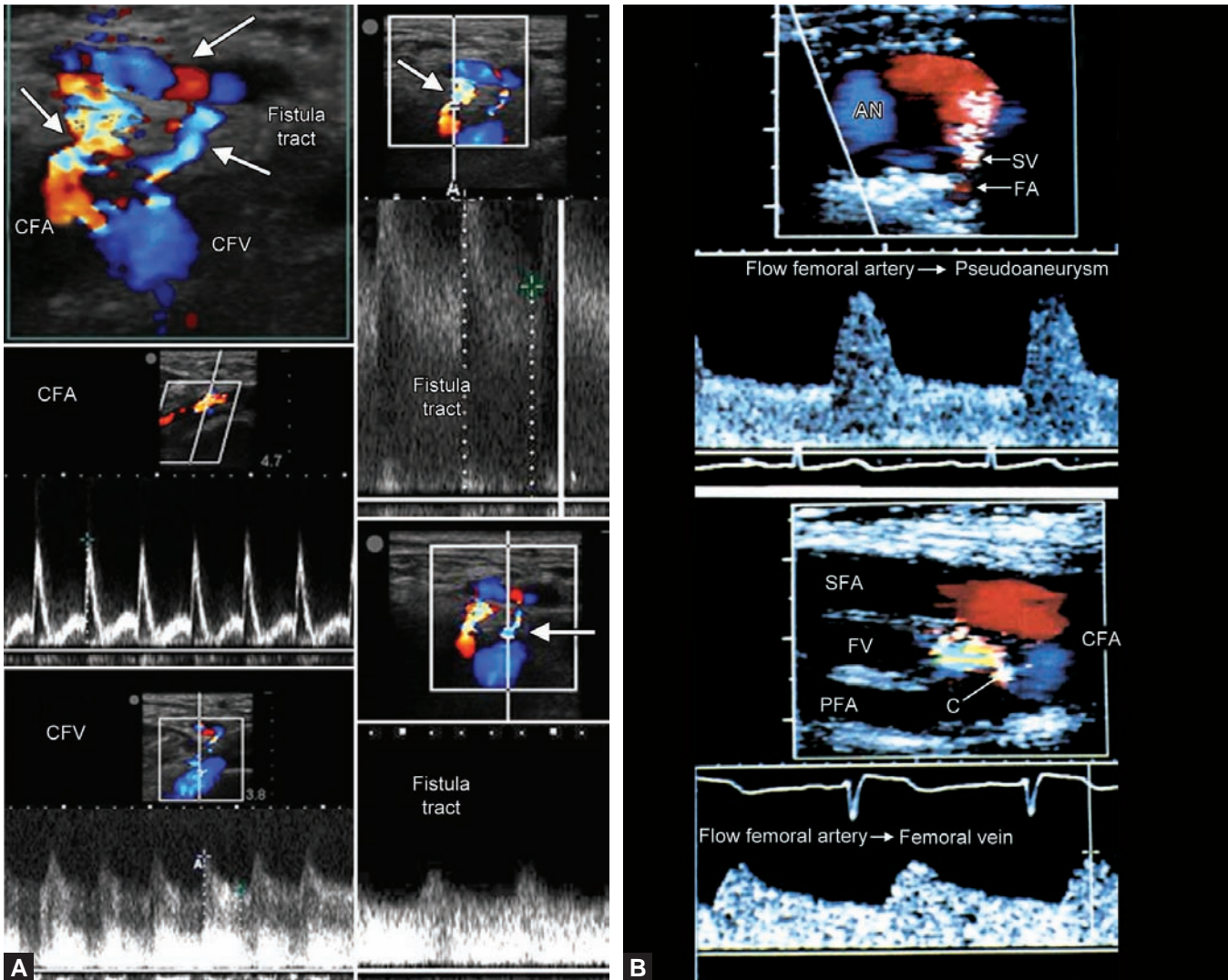
Small fistulas may close spontaneously in a short period of time, but larger communications may require percutaneous closure with covered stents or undergo surgical repair^{74,76} (Figs 33.32A and B).

Dissection rarely occurs in healthy vascular segments, most commonly are seen in atherosclerotic vessels when

puncturing the plaque, and advancing the wire may cause disruption of the plaque. The incidence of dissection has been reported to be approximately 0.4% after cardiac catheterizations, but incidence may be higher considering undiagnosed cases.

If arterial dissection is suspected, Duplex ultrasound will prove useful to confirm the presence of a “dissection flap” in the common femoral artery, and both, the true and the false lumen should be identified.

Nonlimiting flow lesions may heal spontaneously, but flow-limiting dissections or occluded vascular segments should be surgically or percutaneously treated.⁷⁶



Figs 33.32A and B: Arteriovenous (AV) fistula after femoral artery access. (A) Transverse view of the femoral artery and femoral vein demonstrates multiple interconnected tracts after multiple puncture attempts. These tracts create an AV fistula, which exhibits high systolic and diastolic velocity flow in the common femoral artery and vein, and in the interconnected tracts; (B) This color duplex ultrasound exhibits a pseudoaneurysm of the femoral artery and an AV fistula. The presence of a palpable thrill or auscultation of a continuous bruit over the groin should raise concern for coexistent lesions.

(Source: (Fig. 33.32B) Reproduced with permission from Su CT, Nanda NC, Pinheiro L, et al. Combined Femoral Pseudoaneurysm and Arteriovenous Fistula: Diagnosis by Doppler Color Flow Mapping. *Echocardiography*. 1990;7(2):169–75).

REFERENCES

- Gerhard-Herman M, Gardin JM, Jaff M, et al. American Society of Echocardiography; Society of Vascular Medicine and Biology. Guidelines for noninvasive vascular laboratory testing: a report from the American Society of Echocardiography and the Society of Vascular Medicine and Biology. *J Am Soc Echocardiogr*. 2006;19(8):955–72.
- Roman MJ, Naqvi TZ, Gardin JM, et al. American Society of Echocardiography; Society of Vascular Medicine and Biology. Clinical application of noninvasive vascular ultrasound in cardiovascular risk stratification: a report from the American Society of Echocardiography and the Society of Vascular Medicine and Biology. *J Am Soc Echocardiogr*. 2006;19(8):943–54.
- Creager MA, Cooke JP, Olin JW, et al. Society for Cardiovascular Angiography and Interventions; Society for Vascular Medicine. Task force 11: training in vascular medicine and peripheral vascular catheter-based interventions endorsed by the Society for Cardiovascular Angiography and Interventions and the Society for Vascular Medicine. *J Am Coll Cardiol*. 2008;51(3):398–404.

4. Moussa ID, Mohr J. Epidemiology and natural history of asymptomatic carotid artery stenosis. In: Moussa ID, editor. *Asymptomatic Carotid Artery Stenosis*. Informa Healthcare; 2007:1–18.
5. Khurana R, Teal P. Carotid artery stenosis prevalence and medical therapy. In: Saw J, editor. *Carotid Artery Stenting: The Basics*. Contemporary Cardiology. Humana Press; 2009:3–19.
6. Beneficial effect of carotid endarterectomy in symptomatic patients with high-grade carotid stenosis. North American Symptomatic Carotid Endarterectomy Trial Collaborators. *N Engl J Med*. 1991 Aug 15;325(7):445–53. PubMed PMID: 1852179.
7. MRC European Carotid Surgery Trial: interim results for symptomatic patients with severe (70–99%) or with mild (0–29%) carotid stenosis. European Carotid Surgery Trialists' Collaborative Group. *Lancet*. 1991 May 25;337(8752):1235–43. PubMed PMID: 1674060.
8. Endarterectomy for asymptomatic carotid artery stenosis. Executive Committee for the Asymptomatic Carotid Atherosclerosis Study. *JAMA*. 1995 May 10;273(18):1421–8. PubMed PMID: 7723155.
9. AbuRahma AF, Wulu JT Jr, Crotty B. Carotid plaque ultrasonic heterogeneity and severity of stenosis. *Stroke*. 2002;33(7):1772–5.
10. Sidhu PS, Allan PL. The extended role of carotid artery ultrasound. *Clin Radiol*. 1997 Sep;52(9):643–53. PubMed PMID: 9313727.
11. Bates ER, Babb JD, Casey DE Jr, et al. American College of Cardiology Foundation Task Force; American Society of Interventional & Therapeutic Neuroradiology; Society for Cardiovascular Angiography and Interventions; Society for Vascular Medicine and Biology; Society for Interventional Radiology. ACCF/SCAI/SVMB/SIR/ASITN 2007 Clinical Expert Consensus Document on carotid stenting. *Vasc Med*. 2007;12(1):35–83.
12. Layton KE, Kallmes DF, Cloft HJ, et al. Bovine aortic arch variant in humans: clarification of a common misnomer. *AJNR Am J Neuroradiol*. 2006;27(7):1541–2.
13. Fisher RG, Whigham CJ, Trinh C. Diverticula of Kommerell and aberrant subclavian arteries complicated by aneurysms. *Cardiovasc Intervent Radiol*. 2005;28(5):553–60.
14. Sachar R, Kapadia S. Cerebrovascular anatomy. In: Saw J, Exaire JE, Lee D, Yadav J, editors. *Handbook Of Complex Percutaneous Carotid Intervention*. Contemporary Cardiology. Humana Press; 2007:65–82.
15. Berguer R, Kieffer E. The Aortic Arch and Its Branches: Anatomy and Blood Flow. *Surgery of the Arteries to the Head*. New York: Springer; 1992:5–31.
16. AbuRahma A. Overview of Cerebrovascular Disease. In: AbuRahma A, Bergan J, editors. *Noninvasive Vascular Diagnosis*. London: Springer; 2007:33–49.
17. Lynn R, Abou-Chebl A. Cerebral Arterial Anatomy. In: Macdonald S, Stansby G, editors. *Practical Carotid Artery Stenting*. London: Springer; 2009:63–74.
18. Saw J, Walsh S. Aortic arch and cerebrovascular anatomy and angiography. In: Saw J, editor. *Carotid Artery Stenting: The Basics*. Contemporary Cardiology. Humana Press; 2009:149–69.
19. Polak J. Normal cerebrovascular anatomy and collateral pathways. In: Pellerito J, editor. *Introduction to Vascular Ultrasonography*. 6th ed. Elsevier; 2012:128–35.
20. Horrow MM, Stassi J. Sonography of the vertebral arteries: a window to disease of the proximal great vessels. *AJR Am J Roentgenol*. 2001;177(1):53–9.
21. Polak J. Normal findings and technical aspects of carotid sonography. In: Pellerito J, editor. *Introduction to Vascular Ultrasonography*. 6th ed. Elsevier; 2012:136–46.
22. Rohren EM, Kliewer MA, Carroll BA, et al. A spectrum of Doppler waveforms in the carotid and vertebral arteries. *AJR Am J Roentgenol*. 2003;181(6):1695–704.
23. Touboul PJ, Hennerici MG, Meairs S, et al. Mannheim carotid intima-media thickness consensus (2004–2006). An update on behalf of the Advisory Board of the 3rd and 4th Watching the Risk Symposium, 13th and 15th European Stroke Conferences, Mannheim, Germany, 2004, and Brussels, Belgium, 2006. *Cerebrovasc Diseases*. 2007;23(1):75–80. PubMed PMID: 17108679.
24. Stein JH, Korcarz CE, Hurst RT, et al. Use of carotid ultrasound to identify subclinical vascular disease and evaluate cardiovascular disease risk: a consensus statement from the American Society of Echocardiography Carotid Intima-Media Thickness Task Force. Endorsed by the Society for Vascular Medicine. *J Am Soc Echocardiogr*. 2008 Feb;21(2):93–111; quiz 89–90. PubMed PMID: 18261694.
25. Bots M, Peters SE, Grobbee D. Carotid intima-media thickness measurement: a suitable alternative for cardiovascular risk? In: Nicolaides A, Beach KW, Kyriacou E, Pattichis CS, editors. *Ultrasound and Carotid Bifurcation Atherosclerosis*. London: Springer; 2012:379–95.
26. To T-D, Naqvi T. Intima-Media Thickness and Carotid Plaques in Cardiovascular Risk Assessment. In: Nicolaides A, Beach KW, Kyriacou E, Pattichis CS, editors. *Ultrasound and Carotid Bifurcation Atherosclerosis*. London: Springer; 2012:397–418.
27. Salonen JT, Salonen R. Ultrasound B-mode imaging in observational studies of atherosclerotic progression. *Circulation*. 1993;87(3 Suppl):II56–II65.
28. O'Leary DH, Polak JF, Kronmal RA, et al. Carotid-artery intima and media thickness as a risk factor for myocardial infarction and stroke in older adults. Cardiovascular Health Study Collaborative Research Group. *N Engl J Med*. 1999;340(1):14–22.
29. Lorenz MW, Markus HS, Bots ML, et al. Prediction of clinical cardiovascular events with carotid intima-media thickness: a systematic review and meta-analysis. *Circulation*. 2007;115(4):459–67.
30. Chambless LE, Heiss G, Folsom AR, et al. Association of coronary heart disease incidence with carotid arterial wall thickness and major risk factors: the Atherosclerosis Risk in Communities (ARIC) Study, 1987–1993. *Am J Epidemiol*. 1997 Sep 15;146(6):483–94. PubMed PMID: 9290509.
31. Lorenz MW, von Kegler S, Steinmetz H, et al. Carotid intima-media thickening indicates a higher vascular

- risk across a wide age range: prospective data from the Carotid Atherosclerosis Progression Study (CAPS). *Stroke*. 2006;37(1):87–92.
32. Johnsen SH, Mathiesen EB, Joakimsen O, et al. Carotid atherosclerosis is a stronger predictor of myocardial infarction in women than in men: a 6-year follow-up study of 6226 persons: the Tromsø Study. *Stroke*. 2007; 38(11):2873–80.
 33. Hofman A, Grobbee DE, de Jong PT, et al. Determinants of disease and disability in the elderly: the Rotterdam Elderly Study. *Eur J Epidemiol*. 1991 Jul;7(4):403–22. PubMed PMID: 1833235.
 34. Polak JF, Pencina MJ, Pencina KM, et al. Carotid-wall intima-media thickness and cardiovascular events. *N Engl J Med*. 2011;365(3):213–21.
 35. Hall H, Bassiouny H. Pathophysiology of Carotid Atherosclerosis. In: Nicolaidis A, Beach KW, Kyriacou E, Pattichis CS, editors. *Ultrasound and Carotid Bifurcation Atherosclerosis*: London: Springer; 2012:27–39.
 36. Bluth EI, Stavros AT, Marich KW, et al. Carotid duplex sonography: a multicenter recommendation for standardized imaging and Doppler criteria. *Radiographics*. 1988; 8(3):487–506.
 37. Spence JD, Eliasziw M, DiCicco M, et al. Carotid plaque area: a tool for targeting and evaluating vascular preventive therapy. *Stroke*. 2002;33(12):2916–22.
 38. Polak JF, Shemanski L, O’Leary DH, et al. Hypoechoic plaque at US of the carotid artery: an independent risk factor for incident stroke in adults aged 65 years or older. *Cardiovascular Health Study*. *Radiology*. 1998;208(3): 649–54.
 39. Honda O, Sugiyama S, Kugiyama K, et al. Echolucent carotid plaques predict future coronary events in patients with coronary artery disease. *J Am Coll Cardiol*. 2004; 43(7):1177–84.
 40. Nandalur KR, Baskurt E, Hagspiel KD, et al. Calcified carotid atherosclerotic plaque is associated less with ischemic symptoms than is noncalcified plaque on MDCT. *AJR Am J Roentgenol*. 2005;184(1):295–8.
 41. Geroulakos G, Ramaswami G, Nicolaidis A, et al. Characterization of symptomatic and asymptomatic carotid plaques using high-resolution real-time ultrasonography. *Br J Surg*. 1993;80(10):1274–7.
 42. Bekelis K LN, Griffin M, Nicolaidis A. Grading Internal Carotid Artery Stenosis. In: A N, editor. *Ultrasound and Carotid Bifurcation Atherosclerosis*: Springer; 2012:521–42.
 43. Nicolaidis AN, Shifrin EG, Bradbury A, et al. Angiographic and duplex grading of internal carotid stenosis: can we overcome the confusion? *J Endovasc Surg*. 1996;3(2): 158–65.
 44. Taylor DC, Strandness DE Jr. Carotid artery duplex scanning. *J Clin Ultrasound*. 1987;15(9):635–44.
 45. Zwiebel WJ. Spectrum analysis in carotid sonography. *Ultrasound Med Biol*. 1987;13(10):625–36.
 46. Grant EG, Benson CB, Moneta GL, et al. Carotid artery stenosis: gray-scale and Doppler US diagnosis—Society of Radiologists in Ultrasound Consensus Conference. *Radiology*. 2003;229(2):340–6.
 47. Grant EG, Duerinckx AJ, El Saden SM, et al. Ability to use duplex US to quantify internal carotid arterial stenoses: fact or fiction? *Radiology*. 2000;214(1):247–52.
 48. Spencer MP, Reid JM. Quantitation of carotid stenosis with continuous-wave (C-W) Doppler ultrasound. *Stroke*. 1979;10(3):326–30.
 49. AbuRahma AF, Srivastava M, Stone PA, et al. Critical appraisal of the Carotid Duplex Consensus criteria in the diagnosis of carotid artery stenosis. *J Vasc Surg*. 2011 Jan;53(1):53–9; discussion 9–60. PubMed PMID: 20951536.
 50. Tahmasebpour HR, Buckley AR, Cooperberg PL, et al. Sonographic examination of the carotid arteries. *Radiographics*. 2005;25(6):1561–75.
 51. Alexandrov A, Colognori D, Shu MD, et al. Human spliceosomal protein CWC22 plays a role in coupling splicing to exon junction complex deposition and nonsense-mediated decay. *Proc Natl Acad Sci USA*. 2012; 109(52):21313–8.
 52. AbuRahma A. Duplex scanning of the extracranial carotid arteries. In: AbuRahma A, editor. *Noninvasive Vascular Diagnosis A Practical Guide to Therapy*. Springer; 2013: 79–109.
 53. AbuRahma AF, Richmond BK, Robinson PA, et al. Effect of contralateral severe stenosis or carotid occlusion on duplex criteria of ipsilateral stenoses: comparative study of various duplex parameters. *J Vasc Surg*. 1995;22(6):751–61; discussion 761.
 54. Hayes AC, Johnston KW, Baker WH, et al. The effect of contralateral disease on carotid Doppler frequency. *Surgery*. 1988;103(1):19–23.
 55. Ray SA, Lockhart SJ, Dourado R, et al. Effect of contralateral disease on duplex measurements of internal carotid artery stenosis. *Br J Surg*. 2000;87(8):1057–62.
 56. Forconi S, Johnston KW. Effect of contralateral internal carotid stenosis on the accuracy of continuous wave Doppler spectral analysis results. *J Cardiovasc Surg (Torino)*. 1987;28(6):715–8.
 57. Wholey MH, Wholey MH. History and current status of endovascular management for the extracranial carotid and supra-aortic vessels. *J Endovasc Therapy*. 2004 Dec;11 Suppl 2:II43–61. PubMed PMID: 15760247.
 58. Brott TG, Hobson RW 2nd, Howard G, et al. CREST Investigators. Stenting versus endarterectomy for treatment of carotid-artery stenosis. *N Engl J Med*. 2010;363(1):11–23.
 59. Thomas M, Otis SM, Rush M, et al. Recurrent carotid artery stenosis following endarterectomy. *Ann Surg*. 1984; 200(1):74–9.
 60. Mattos MA, Shamma AR, Rossi N, et al. Is duplex follow-up cost-effective in the first year after carotid endarterectomy? *Am J Surg*. 1988;156(2):91–5.
 61. Ouriel K, Green RM. Appropriate frequency of carotid duplex testing following carotid endarterectomy. *Am J Surg*. 1995;170(2):144–7.
 62. Aburahma AF. Duplex criteria for determining 50% and 80% internal carotid artery stenosis following carotid endarterectomy with patch angioplasty. *Vascular*. 2011; 19(1):15–20.

63. AbuRahma AF, Maxwell D, Eads K, et al. Carotid duplex velocity criteria revisited for the diagnosis of carotid in-stent restenosis. *Vascular*. 2007;15(3):119-25.
64. AbuRahma AF, Abu-Halimah S, Bensenhaver J, et al. Optimal carotid duplex velocity criteria for defining the severity of carotid in-stent restenosis. *J Vasc Surg*. 2008;48(3):589-94.
65. Lal BK, Hobson RW 2nd, Tofighi B, et al. Duplex ultrasound velocity criteria for the stented carotid artery. *J Vasc Surg*. 2008;47(1):63-73.
66. Kepplinger J, Barlinn K, Alexandrov A. Vertebral Artery Ultrasonography. In: AbuRahma AF, Bandyk DF, editors. *Noninvasive Vascular Diagnosis*. London, Springer; 2013:123-31.
67. Schäberle W. Extracranial Cerebral Arteries. *Ultrasonography in Vascular Diagnosis*. Berlin Heidelberg: Springer; 2011:291-375.
68. Kalaria VG, Jacob S, Irwin W, et al. Duplex ultrasonography of vertebral and subclavian arteries. *J Am Soc Echocardiogr*. 2005;18(10):1107-11.
69. Kliewer MA, Hertzberg BS, Kim DH, et al. Vertebral artery Doppler waveform changes indicating subclavian steal physiology. *AJR Am J Roentgenol*. 2000;174(3):815-9.
70. O'Boyle MK, Vibhakar NI, Chung J, et al. Duplex sonography of the carotid arteries in patients with isolated aortic stenosis: imaging findings and relation to severity of stenosis. *AJR Am J Roentgenol*. 1996;166(1):197-202.
71. Kervancioglu S, Davutoglu V, Ozkur A, et al. Duplex sonography of the carotid arteries in patients with pure aortic regurgitation: pulse waveform and hemodynamic changes and a new indicator of the severity of aortic regurgitation. *Acta Radiol*. 2004 Jul;45(4):411-6. PubMed PMID: 15323393.
72. Wood MM, Romine LE, Lee YK, et al. Spectral Doppler signature waveforms in ultrasonography: a review of normal and abnormal waveforms. *Ultrasound Q*. 2010;26(2):83-99.
73. Cervini P, Park SJ, Shah DK, et al. Carotid Doppler ultrasound findings in patients with left ventricular assist devices. *Ultrasound Q*. 2010;26(4):255-61.
74. Ramee S. Chapter 16 Vascular access complications and treatment. In: Jaff M, editor. *Vascular Disease*. Cardiotext; 2011:309-25.
75. Bhatti S, Cooke R, Shetty R, et al. Femoral vascular access-site complications in the cardiac catheterization laboratory: diagnosis and management. *Interven Cardiol*. 2011 2011/08/01;3(4):503-14.
76. Cragen D, Heuser R. Complications of peripheral interventions. *Textbook of Peripheral Vascular Interventions*. 789-98.
77. Schillinger M. Arterial and venous access site complications. *Complications in Peripheral Vascular Interventions*. 49-70.
78. Wiley JM, White CJ, Uretsky BF. Noncoronary complications of coronary intervention. *Catheter Cardiovasc Interv*. 2002;57(2):257-65.
79. Chatterjee T, Do DD, Kaufmann U, et al. Ultrasound-guided compression repair for treatment of femoral artery pseudoaneurysm: acute and follow-up results. *Cathet Cardiovasc Diagn*. 1996;38(4):335-40.
80. Popma JJ, Satler LF, Pichard AD, et al. Vascular complications after balloon and new device angioplasty. *Circulation*. 1993;88(4 Pt 1):1569-78.
81. Schaub F, Theiss W, Busch R, et al. Management of 219 consecutive cases of postcatheterization pseudoaneurysm. *J Am Coll Cardiol*. 1997;30(3):670-5.
82. Katzenschlager R, Ugurluoglu A, Ahmadi A, et al. Incidence of pseudoaneurysm after diagnostic and therapeutic angiography. *Radiology*. 1995;195(2):463-6.
83. Stone P, Campbell J, II. Duplex Ultrasound in the Evaluation and Management of Post-Catheterization Femoral Pseudoaneurysms. In: AbuRahma AF, Bandyk DF, editors. *Noninvasive Vascular Diagnosis*. London: Springer; 2013:347-53.
84. Coughlin BF, Paushter DM. Peripheral pseudoaneurysms: evaluation with duplex US. *Radiology*. 1988;168(2):339-42.
85. Zierler E. Chapter 26—Evaluation and treatment of femoral pseudoaneurysms. In: Zierler E, editor. *Strandness's Duplex Scanning in Vascular Disorders*. Lippincott Williams & Wilkins; 2010.
86. Webber GW, Jang J, Gustavson S, et al. Contemporary management of postcatheterization pseudoaneurysms. *Circulation*. 2007;115(20):2666-74.
87. Toursarkissian B, Allen BT, Petrinc D, et al. Spontaneous closure of selected iatrogenic pseudoaneurysms and arteriovenous fistulae. *J Vasc Surg*. 1997;25(5):803-8; discussion 808.
88. Fellmeth BD, Roberts AC, Bookstein JJ, et al. Post-angiographic femoral artery injuries: nonsurgical repair with US-guided compression. *Radiology*. 1991;178(3):671-5.
89. Coley BD, Roberts AC, Fellmeth BD, et al. Postangiographic femoral artery pseudoaneurysms: further experience with US-guided compression repair. *Radiology*. 1995;194(2):307-11.
90. Eisenberg L, Paulson EK, Kliewer MA, et al. Sonographically guided compression repair of pseudoaneurysms: further experience from a single institution. *AJR Am J Roentgenol*. 1999;173(6):1567-73.
91. Cope C, Zeit R. Coagulation of aneurysms by direct percutaneous thrombin injection. *AJR Am J Roentgenol*. 1986;147(2):383-7.
92. Paulson EK, Sheafor DH, Kliewer MA, et al. Treatment of iatrogenic femoral arterial pseudoaneurysms: comparison of US-guided thrombin injection with compression repair. *Radiology*. 2000;215(2):403-8.